Stimulated electromagnetic shock radiation: Classical second-order calculations

A. A. Risbud* and N. C. Kamerkar†
Department of Physics, University of Pune, Pune 411 007, India
(Received 18 January 2000; revised manuscript received 21 September 2000; published 22 February 2001)

By performing classical, relativistic, second-order calculations we have shown that simulated electromagnetic shock radiation (SESR) is given out as an enormously amplified, exponentially growing, frequency upshifted, highly directional coherent electromagnetic radiation. We have derived expressions specifying the electric field components of SESR in the most compact and readable form. Hence we have calculated the field amplitudes of SESR for different sets of external controlling parameters and plotted some typical results in the most sensitive region, viz., very near the threshold of superphase motion. We have also shown the variation of SESR with respect to external parameters graphically. The results obtained are of importance in achieving a tunable source of coherent radiation in the frequency region not covered by existing sources.

DOI: 10.1103/PhysRevE.63.036501 PACS number(s): 41.60.Cr, 41.60.Bq

I. INTRODUCTION

The interaction in a medium of an electromagnetic wave and a relativistic electron beam possessing superluminal velocity (exceeding the phase velocity of the electromagnetic waves in that medium) has been considered by many workers so far [1–13]. A charged particle traversing a dielectric with superluminal velocity emits Cherenkov radiation [14]. It is the well known process of spontaneous Cherenkov radiation that has been extensively studied [15,16] both experimentally and theoretically. When the charged particle possessing superluminal velocity is additionally kept under the influence of an external electromagnetic wave, it gets modulated and hence emits stimulated Cherenkov radiation [17]. The currently developing devices of coherent electromagnetic radiation, viz., Cherenkov free-electron lasers [18], are based on the process of stimulated Cherenkov radiation. Stimulated electromagnetic shock radiation, the subject of the present paper, is a special case of stimulated Cherenkov radiation in which a particular geometry, viz., head-on collision of an electron beam and an electromagnetic wave, is considered. It is of interest from the theoretical as well as the experimental point of view because of its possible use for generating coherent electromagnetic radiation in the frequency region not covered by existing sources.

Schneider and Spitzer proposed [1] a mechanism for producing coherent photons by interaction in a dispersive nonabsorbing medium of relativistic electrons having superluminal velocity with counterflowing coherent electromagnetic waves, and named [2] the effect *stimulated electromagnetic shock radiation* (SESR) [19]. In a series of interesting papers [1–6] they studied and discussed the properties of SESR. It involves a synergism between two known phenomena, namely, the Doppler shift in frequency of Compton backscattering from relativistic electrons in vacuum [20] and the formation of a shock by a material body moving at a speed greater than that of the waves it produces in the medium. It comprises the generation of intense radiation in the form of a shock front, with frequencies shifted markedly from that of the incident wave. The emitted radiation is claimed to be very intense, coherent, and highly directional, and of frequency that is greatly upshifted from that of the incident electromagnetic wave. Moreover, it is tunable, i.e., the output characteristics of the radiation can be varied over a wide range of parameters obtainable by changing any one or any combination of characteristics of three physical agents that produce this effect. They are the incident electromagnetic wave, the electron beam, and the polarizable medium. Because of these striking features the effect seems to be very interesting and useful for achieving a better, tunable source of coherent electromagnetic radiation of frequency not available at present.

However, the results obtained by Schneider and Spitzer have some limitations. They used many simplifying approximations such as the use of the electron's mean position and mean energy instead of using their time varying values explicitly. They considered only the first-order electric field effects and omitted the magnetic field effects which actually become significant for the electron ultrarelativistic motion. Without working out the interaction process rigorously by incorporating higher order calculations for the simplest case of dispersionless dielectrics, they have extended their, rather approximate, analysis to more complicated situations of dispersive and active media. Therefore their claims about SESR, such as directionality, coherence, orders of magnitude enhancement over ordinary Cherenkov radiation, and a significant frequency upshift compared to the incident electromagnetic wave, need to be checked with more rigorous calculations. Further theoretical work on this effect by Soln [9], Zachary [7,10], Kroll [8], Becker [12], and Risbud [13] did not support most of the conclusions of Schneider and Spitzer and exhibited somewhat contradictory results. Zachary's results implied the requirement of an extension of the present linear theory to second order or higher to take into account recoil of the radiating particle. Becker's quantum mechanical treatment [12] also concluded that a linear approximation with respect to the intensity of the incident field is not sufficient for Cherenkov type SESR.

All the above mentioned dynamical calculations were confined to linear response of the electron to the incident

*Electronic address: risbud@physics.unipune.ernet.in
†Electronic address: nck@unipune.ernet.in

wave and the analysis needs to be supplemented by the study of nonlinear effects such as the effect of the recoil of the electron (which is due to the effect of the magnetic field **B** associated with the incident electromagnetic wave) on the radiation. The effect is intrinsically classical and the calculations involve only Maxwell's equations and the Lorentz force equation in a polarizable medium. Because of the importance of the effect we have done the calculations introducing second-order electric field effects on SESR. For simplicity, we have restricted consideration to a nonmagnetic dispersionless dielectric medium, although the dispersive nature of the dielectric is expected to play an important role in SESR.

In this paper we present our work in the following five sections. In Sec. II we give a general outline of the method by which we have tackled the problem mathematically. In Sec. III, we outline the major steps involved in the calculations and discuss the meaning of the main results of our present work specified by Eqs. (26), (27), and (28) below representing the electric field components of SESR, and compare them with the results of previous works. As the results expressed by Eqs. (26)–(28) are not suitable for calculating the field strengths of SESR, we have performed in Sec. IV an integration with respect to ω and obtained the results in nice, compact, and readable form as given by Eqs. (35), (36), and (37). These expressions are more suitable for numerical calculations of the field components and they also exhibit all the characteristics of SESR. We have also calculated the field strengths of SESR by varying the parameters in their entire feasible ranges. Section IV is devoted to numerical estimates and their analysis. In Sec. V the graphical representation of the numerical calculations of the results is shown by Figs. 1–10. Section VI is devoted to a summary and conclusions.

II. GENERAL OUTLINE

In this paper, by using the method of Fourier transforms, we have obtained the second-order solutions (nonlinear response of the electron to the incident wave) of Maxwell's equations that specify the electromagnetic fields that generate SESR in the configuration of a linearly polarized plane electromagnetic wave (of amplitudes $\mathbf{E}_0, \mathbf{B}_0$ and frequency ω_0) colliding head on with a relativistic electron beam possessing superluminal velocity $\mathbf{v}_0$ ($v_0 > c/n_0$, $n_0 = \sqrt{\epsilon\mu}$ = refractive index) along the Z axis in a nonmagnetic homogeneous isotropic linear dispersionless dielectric medium of infinite extent. We assume that the electron's velocity is just above (i.e., very much in the vicinity of) the threshold of superphase motion. We have used standard notation and Gaussian units throughout this paper. Using Fourier transforms of all quantities, namely, **E**, **B**, ρ, and **j**, appearing in Maxwell's equations, their general solutions are written as [13]

$$\mathbf{E}(\mathbf{X},t) = \frac{4\pi i}{(2\pi)^4}\int_{-\infty}^{+\infty} d^3k\, d\omega \times e^{i(\omega t - \mathbf{k}\cdot\mathbf{X})}\frac{[\omega \mathbf{j}(\mathbf{k},\omega) - c^2\mathbf{k}\rho(\mathbf{k},\omega)/\epsilon]}{\omega^2\epsilon - c^2k^2}, \quad (1)$$

$$\mathbf{B}(\mathbf{X},t) = \frac{-4\pi c}{(2\pi)^4}\nabla \times \int_{-\infty}^{+\infty} d^3k\, d\omega\, e^{i(\omega t - \mathbf{k}\cdot\mathbf{X})}\left[\frac{\mathbf{j}(\mathbf{k},\omega)}{\omega^2\epsilon - c^2k^2}\right]. \quad (2)$$

These equations are general in so far as external sources (**j**, ρ) are concerned, i.e., they hold for an arbitrary charge distribution of electrons in the incident beam.

In order to determine electromagnetic fields we have performed the complicated multiple integrals appearing in Eqs. (1) and (2) with the substitution of the driving terms, viz., $\rho(\mathbf{k},\omega)$ and $\mathbf{j}(\mathbf{k},\omega)$, appropriate for the situation under study. For that we have calculated Fourier transforms of the charge density $\rho(\mathbf{R},t)$ and the current density $\mathbf{j}(\mathbf{R},t)$ by first determining the time varying velocity $\mathbf{V}(t)$ and the position $\mathbf{R}(t)$ of the electron under the influence of the incident electromagnetic wave by solving the Lorentz force equation that governs the electron's motion.

III. CALCULATIONS

In the following we consider the electromagnetic wave interacting as a whole with the electron (single particle interaction). Therefore, we retain in addition to the electric field term the magnetic field term in the Lorentz force equation. The effect of the magnetic field is seen to induce recoil in the electron's motion. We have done the second-order calculations by retaining terms up to E_0^2 which are sufficient to include magnetic field effects. We have taken the electron's time varying position and energy explicitly in the calculations and used relativistically correct equations throughout. However, in our expression the magnetic field is not explicitly seen as we have expressed it in terms of the electric field associated with the electromagnetic wave.

In the situation under consideration, with respect to the laboratory frame of reference, we write the charge and current densities respectively as

$$\rho(\mathbf{r},t) = -e\,\delta(\mathbf{r} - \mathbf{R}(t)), \quad (3)$$

$$\mathbf{j}(\mathbf{r},t) = -e\mathbf{V}(t)\,\delta(\mathbf{r} - \mathbf{R}(t)), \quad (4)$$

where δ denotes the Dirac δ function, e is the magnitude of the electronic charge, $\mathbf{V}(t) = d\mathbf{R}(t)/dt$, $\mathbf{R}(t)$ is the position of the electron at time t in the field of the incident electromagnetic wave, and $\mathbf{r}$ is the position of an observer at time t. The Lorentz force on the electron due to the incident electromagnetic wave in a medium [21,22] is

$$\mathbf{F} = \frac{d}{dt}(\gamma m_0 \mathbf{V}) = -e\left[\mathbf{E}_i(\mathbf{R},t) + \frac{\mathbf{V}}{c}\times(\mathbf{B}_i(\mathbf{R},t))\right]\gamma\epsilon, \quad (5)$$

where m_0 is the rest mass of an electron, $\gamma = (1 - V^2/c^2)^{-1/2}$,

$$\mathbf{E}_i = \mathbf{E}_0 \sin(\omega_0 t - k_0 z) = \hat{y}E_i \quad (6)$$

and

$$\mathbf{B}_i = \mathbf{B}_0 \sin(\omega_0 t - k_0 z) = \hat{x}B_i \quad (7)$$

are, respectively, the electric and magnetic fields of the incident electromagnetic wave at the electron's position, and

$$\mathbf{B}_i = n_0 \hat{k}_0 \times \mathbf{E}_i, \quad \hat{k}_0 = \frac{\mathbf{k}_0}{|\mathbf{k}_0|} = -\hat{z}, \quad |\mathbf{k}_0| = \frac{\omega_0 n_0}{c}. \tag{8}$$

Due to the relativistic anomalous Doppler effect [23,24] the frequency of the electromagnetic wave experienced by the electron is

$$\Omega = \frac{\gamma_0 \omega_0 (1+\beta_0 n_0)}{\beta_0 n_0 \cos\theta_0 - 1}, \tag{9}$$

where $\beta_0 = |\mathbf{v}_0/c|$, $\gamma_0 = (1-\beta_0^2)^{-1/2}$, and θ_0 is the observation angle measured with respect to the electron velocity direction. We assume that the initial velocity of the electron is very slightly above the threshold value for superphase motion. We seek the solutions of the Lorentz force equation (5) in the form [25]

$$v_z = \frac{c}{n_0}(1+\mu u_z), \quad v_y = \frac{c}{n_0}\mu u_y, \quad v_x = 0, \tag{10}$$

where $\mu \ll 1$ and $\mathbf{v}|_{t=0} = \mathbf{v}_0$, because of the boundary conditions, viz., $u_z|_{t=0} = 1$, $u_y|_{t=0} = 0$. Using Eq. (10) in Eq. (5) and linearizing with respect to μ we get [26] the electron's velocity as

$$v_y = -b_0 \sin 2\Omega t, \quad v_z = v_0 + v_z', \tag{11}$$

where $v_z' = a_0(\cos 4\Omega t - 1)$, $a_0 = cfd/16\Omega^2 n_0$, and $b_0 = cd/2\Omega n_0$.

The velocity of the electron in the inertial frame moving with velocity $\mathbf{v}_0$ with respect to the laboratory is $(0, v_y, v_z')$. Transforming to the laboratory frame of reference, using the Lorentz transformation equation [24], we get the electron's velocity and position, respectively, as

$$\mathbf{V}(t) = \left(0, \frac{v_y}{\gamma_0}, v_0 + \frac{v_z'}{\gamma_0^2}\right) \tag{12}$$

and

$$\mathbf{R}(t) = \left(0, \frac{1}{\gamma_0} y(t), v_0 t + \frac{1}{\gamma_0^2} z(t)\right) \tag{13}$$

where $y(t) = \int v_y(t)dt$ and $z(t) = \int v_z'(t)dt$.

Substituting v_y and v_z from Eq. (11) in Eqs. (12) and (13) and integrating with respect to t we get the following components for the velocity $\mathbf{V}(t)$ and position $\mathbf{R}(t)$ of the electron with respect to the laboratory frame:

$$V_x(t) = 0, \quad V_y(t) = -\frac{b_0}{\gamma_0}\sin 2\Omega t,$$
$$V_z(t) = v_0 + \frac{a_0}{\gamma_0^2}(\cos 4\Omega t - 1) \tag{14}$$

and

$$X(t) = 0, \quad Y(t) = b\cos 2\Omega t, \quad Z(t) = v_0' t + a \sin 4\Omega t, \tag{15}$$

where $a = a_0/\gamma_0^2 4\Omega$, $b = b_0/2\Omega\gamma_0$, and $v_0' = v_0 - 4a\Omega$.

To calculate inverse Fourier transforms of the charge and current densities we use the definition of the inverse Fourier transform as

$$\rho(\mathbf{k},\omega) = \int_{-\infty}^{+\infty}\int_{-\infty}^{+\infty}\int_{-\infty}^{+\infty}\int_{-\infty}^{+\infty} dt\,dx\,dy\,dz\,\rho(\mathbf{r},t)e^{-i(\omega t - \mathbf{k}\cdot\mathbf{r})} \tag{16}$$

and

$$\mathbf{j}(\mathbf{k},\omega) = \int_{-\infty}^{+\infty}\int_{-\infty}^{+\infty}\int_{-\infty}^{+\infty}\int_{-\infty}^{+\infty} dt\,dx\,dy\,dz\,\mathbf{j}(\mathbf{r},t)e^{-i(\omega t - \mathbf{k}\cdot\mathbf{r})}. \tag{17}$$

We use the components of $\mathbf{R}(t)$ and $\mathbf{V}(t)$ from Eqs. (15) and (14) in Eqs. (3) and (4), substitute $\rho(\mathbf{r},t)$ and $\mathbf{j}(\mathbf{r},t)$ thus obtained in Eqs. (16) and (17), and perform the integrals with respect to x, y, z, and t appearing therein using the properties of the δ function and the following relations for the Bessel functions [27]:

$$\exp(\pm ia\sin\theta) = \sum_{l=-\infty}^{+\infty} J_l(a)\exp(\pm il\theta), \tag{18}$$

$$\exp(\pm ia\cos\theta) = \sum_{m=-\infty}^{+\infty} J_m(a)\exp(\pm im\theta)(\pm i)^m. \tag{19}$$

We obtain the following expression for the transformed densities:

$$\rho(\mathbf{k},\omega) = -2\pi e \sum_{l,m=-\infty}^{+\infty} e^{\pi i l/2} J_l(bk_y) J_m(ak_z) \times \delta(\omega - k_z v_0' - 2\Omega(l+2m)), \tag{20}$$

$$j_y(\mathbf{k},\omega) = \pi e b \Omega \sum_{l,m=-\infty}^{+\infty} e^{(i\pi/2)(l-1)} J_l(bk_y) J_m(ak_z) \times [\delta(\omega - k_z v_0' - 2\Omega(l+2m+1)) - \delta(\omega - k_z v_0' - 2\Omega(l+2m-1))], \tag{21}$$

$$j_x(\mathbf{k},\omega) = 0, \quad j_z(\mathbf{k},\omega) = j_0 + j_1, \tag{22}$$

where

$$j_0 = -2\pi e v_0' \sum_{l,m=-\infty}^{+\infty} e^{(\pi i l/2)} J_l(bk_y) J_m(ak_z) \times \delta(\omega - k_z v_0' - 2\Omega(l+2m)), \tag{23}$$

$$j_1 = -4\pi e a \Omega \sum_{l,m=-\infty}^{+\infty} e^{(\pi i l/2)} J_l(bk_y) J_m(ak_z) [\delta(\omega - k_z v_0' - 2\Omega(l+2m+2)) + \delta(\omega - k_z v_0' - 2\Omega(l+2m-2))]. \tag{24}$$

The transformed densities given by Eqs. (20)–(24) are the driving terms in Eqs. (1) and (2). The most important part of the calculations starts here. To determine the electromagnetic fields in the situation under study we have to substitute the values of $\rho(\mathbf{k},\omega)$ and $\mathbf{j}(\mathbf{k},\omega)$ specified by Eqs. (20)–(24) into Eqs. (1) and (2) taken componentwise and perform the multiple integrals appearing therein. We give the details of the calculations in Appendix B. The parameters appearing in Eq. (15), viz., $b = eE_0 n_0 \sqrt{n_0^2 - 1}\,\gamma / 2\Omega^2 m_0 \gamma_0$ and $a = e^2 E_0^2 n_0 (n_0^2 - 1)^2 \gamma^2 / 32 c \Omega^3 m_0^2 \gamma_0^2$ contain all the external controlling factors of the process, the field strength E_0, field frequency ω_0, electron energy γ_0, and refractive index of the medium n_0. In terms of the induced velocity $v_i = eE_0/m_0\Omega$ and $\beta_i = v_i/c$ the parameters b and a can be written as

$$b = \beta_i \frac{c}{\Omega} \frac{n_0 \sqrt{n_0^2 - 1}}{2} \frac{\gamma}{\gamma_0}, \quad a = \beta_i^2 \frac{c}{\Omega} \frac{n_0 (n_0^2 - 1)^2}{32} \frac{\gamma^2}{\gamma_0^2}.$$

We assume that the incident electromagnetic wave is of small intensity (i.e., possessing field strengths considerably less than the breakdown voltages $\approx 10^{10}$ statvolts/cm). Therefore, the dielectric gives a linear response to the fields and the induced velocities are quite small ($\beta_i \leqslant 10^{-3}$). In that case the magnitudes of the parameters b and a are mainly governed by β_i as $b \propto \beta_i$ and $a \propto \beta_i^2$. As $\beta_i \leqslant 10^{-3}$ and $a/b \leqslant 10^{-4}$, we say that b is the first-order parameter in β_i and a is the second-order parameter in β_i (and therefore also in the electric field). It is through these parameters b and a that the interaction of the incident electromagnetic wave with the electron beam has entered into the problem. We note from the expressions of the induced charge and current densities given by Eqs. (20)–(24) that the effect of the external electromagnetic wave is included in the problem through b and a coming from the product of the Bessel functions, viz., $\Sigma_{l,m} J_l(bk_y) J_m(ak_z)$. As $J_l(bk_y) \propto (bk_y)^l$ and $J_m(ak_z) \propto (ak_z)^m$, different powers of the parameters b and a enter into the calculations when the sums with respect to l and m are taken. As the second-order parameter a is at least four orders of magnitude smaller than the first-order parameter b, we neglect the third-order parameter ab as compared to b^2 or a and the fourth-order parameter a^2 as compared to ab, and so on.

Therefore we retain terms containing b, b^2, and a, while neglecting all higher order terms containing $ab, b^3, \ldots$, etc., and $a^2, a^3, \ldots$, etc., in the calculations. For convenience we change to a cylindrical coordinate system with $\mathbf{k}(k_\rho, \phi, k_z)$, $\mathbf{r}(\rho, \phi', z)$, $\mathbf{j}(j_\rho = j_y, j_\phi = 0, j_z)$, $\mathbf{k}\cdot\mathbf{r} = k_\rho \rho \cos(\phi - \phi')$, and $d^3k = k_\rho dk_\rho d\phi\, dk_z$. Using Eq. (1) we write the electric field $\mathbf{E}(E_\rho, E_\phi, E_z)$ as

$$\mathbf{E}(\mathbf{r},t) = \frac{2i}{(2\pi)^3} \int_0^\infty k_\rho dk_\rho \int_0^{2\pi} d\phi \int_{-\infty}^{+\infty} dk_z \int_{-\infty}^{+\infty} d\omega \times e^{i[\omega t - k_\rho \rho \cos(\phi - \phi') - k_s z]} \times \left[\frac{\omega \mathbf{j}(\mathbf{k},\omega) - (c^2\mathbf{k}/\epsilon)\rho(\mathbf{k},\omega)}{\omega^2 \epsilon - c^2 k^2} \right]. \tag{25a}$$

We note that Eq. (25a) written componentwise implies

$$E_z \propto \left[\omega j_z(\mathbf{k},\omega) - \frac{c^2 k_z}{\epsilon} \rho(\mathbf{k},\omega) \right], \tag{25b}$$

$$E_\rho \propto \left[\omega j_\rho(\mathbf{k},\omega) - \frac{c^2 k_\rho}{\epsilon} \rho(\mathbf{k},\omega) \right], \tag{25c}$$

$$E_\phi \propto \frac{c^2 \phi}{\epsilon} \rho(\mathbf{k},\omega), \tag{25d}$$

where the components of the transformed source densities are given by Eqs. (20)–(24). Using relations (25b), (25c), and (25d) we write Eq. (25a) componentwise, perform the multiple integrals appearing therein, make the approximations mentioned, simplify, and obtain [28] the main result specifying the electric field of the emitted radiation as

$$E_z(\mathbf{r},t) = \frac{e}{2c^2} \int \omega\, d\omega\, e^{i\omega t} \Bigg\{ H_0^{(2)}(\rho A) \left(1 - \frac{c^2 k}{\epsilon \omega v_0'} \right) \times \left(1 - \frac{b^2 A^2}{4} \right) e^{-ikz} - H_0^{(2)}(\rho A_\pm) \Bigg[\left(1 - \frac{c^2 k_\pm}{\epsilon \omega v_0'} \right) \times \left(\frac{b^2 A_\pm^2}{8} \pm \frac{a k_\pm}{2} \right) - \frac{2a\Omega}{v_0'} \Bigg] e^{-ik_\pm z} + \frac{b}{2} e^{\mp(\pi i/2)} \times H_0^{(2)}(\rho A_\pm') \left[A_\pm' \left(1 - \frac{c^2 k_\pm'}{\epsilon \omega v_0'} \right) \right] e^{-ik_\pm' z} \Bigg\}, \tag{26}$$

$$E_\rho(\mathbf{r},t) = \frac{e}{2\epsilon v_0'} \int d\omega\, e^{i\omega t} \Bigg\{ -A H_0^{(2)}(\rho A) \left(1 - \frac{b^2 A^2}{4} \right) \times e^{-ikz} + \frac{A_\pm}{2v_0'} H_0^{(2)}(\rho A_\pm) \times \left[\left(\frac{b^2 A_\pm^2}{4} \pm a k_\pm \mp \frac{b^2 \epsilon \Omega}{2c^2} \omega \right) \right] e^{-ik_\pm z} + \frac{b\epsilon}{2} e^{\mp \pi i/2} H_0^{(2)}(\rho A_\pm') \left(\frac{1}{\epsilon} \pm \frac{\Omega}{c^2} \omega \right) e^{-ik_\pm' z} \Bigg\}, \tag{27}$$

and

$$E_\phi(\mathbf{r},t)=\frac{\pi e}{2\epsilon v_0'}\int d\omega\, e^{i\omega t}\Bigg\{H_0^{(2)}(\rho A)\left(1-\frac{b^2A^2}{4}\right)e^{-ikz}+H_0^{(2)}(\rho A_\pm)\left[\left(\frac{b^2A_\pm^2}{8}\pm\frac{ak_\pm}{4}\right)\right]e^{-ik_\pm z}+\frac{b}{2}e^{\mp\pi i/2}A_\pm' H_0^{(2)}(\rho A_\pm')e^{-ik_\pm' z}\Bigg\}, \tag{28}$$

where $\pm$ terms with $\pm$ suffixes are written together for convenience, but are to be read as separate terms, and

$$k=\frac{\omega}{v_0'},\quad A^2=\frac{\epsilon\omega^2}{c^2}-k^2,\quad k_\pm=\frac{\omega_\pm 4\Omega}{v_0'},$$

$$A_\pm^2=\frac{\epsilon\omega^2}{c^2}-k_\pm^2,\quad k_\pm'=\frac{\omega_\pm 2\Omega}{v_0'},$$

$$A_\pm'^2=\frac{\epsilon\omega^2}{c^2}-k_\pm'^2.$$

Equations (26)–(28) are the main results of our present work. They specify the electric field of the emitted radiation in the situation under study. The SESR field is denoted by $\mathbf{E}(E_\rho,E_\phi,E_z)$ where the components E_ρ, E_ϕ, and E_z are given, respectively, by Eqs. (27), (28), and (26). In order to extract the meaning of the main results, it is desirable to simplify these expressions and see how they compare with the results of previous work.

Therefore, we consider a limiting situation, viz., that in which there is no electromagnetic wave, i.e., the situation of ordinary Cherenkov radiation (CR). In that case the field-dependent parameters a and b are zero. Putting $a=b=0$ in Eqs. (26)–(28) we get the components of the electric field of the emitted radiation as

$$E_z(\mathbf{r},t)=\frac{e}{2c^2}\int d\omega\,\omega e^{i(\omega t-kz)}H_0^{(2)}(\rho A_0')\left(1-\frac{1}{\epsilon\beta_0^2}\right), \tag{29}$$

$$E_\rho(\mathbf{r},t)=\frac{-e}{2\epsilon v_0^2}\int d\omega\,\omega e^{i(\omega t-kz)}H_0^{(2)}(\rho A_0')\sqrt{\epsilon\beta_0^2-1}, \tag{30}$$

$$E_\phi(\mathbf{r},t)=\frac{\pi e}{2\epsilon v_0^2}\int d\omega\, e^{i(\omega t-kz)}H_0^{(2)}(\rho A_0'), \tag{31}$$

where

$$A_0'=\frac{\omega}{v_0}\sqrt{\epsilon\beta_0^2-1}.$$

We note that Eqs. (29) and (30) exactly match the result Eqs. 5.1 of Tamm [29], which specify the z and ρ components of the electric field of Cherenkov radiation. The component E_ϕ given by Eq. (31) appears to be additional in our calculations, but it is not so. By substituting the asymptotic value of $H_0^{(2)}(\rho A)$ or otherwise [30,31], the integral appearing in Eq. (31) can be shown to vanish. Thus our result (in the special case of no external electromagnetic wave) exactly reduces to the well known expressions of Tamm [29].

We observe that the terms appearing in our result given by Eqs. (26)–(28) are of two types; viz., Cherenkov-like terms containing the phase factor k, which we call CR-like terms, and terms different from CR containing the phase factor $k_\pm$ and $k_\pm'$, which we identify as true SESR terms. The CR-like components show radiation of frequencies the same as that of CR, but with modified amplitudes, while the true SESR components show a frequency shift. The terms containing a or b^2 specify the second-order field effect. The first-order parameter b is absent in CR-like terms and so the CR-like SESR is a second-order field effect. This conclusion is quite consistent with Eq. (5.27) of Becker [12], in which only second-order terms in intensity of the incident field are seen in the power spectrum. As the treatment of Becker is quantum mechanical, a more exact comparison is not possible. Moreover, Becker omitted the most sensitive region which is very near the threshold, but we have mainly concentrated on that [32]. The SESR components show both the first- and second-order field-induced terms. As CR has no E_ϕ component, getting radiation with E_ϕ given by Eq. (28) is a field-induced effect due to SESR. Moreover, our result, through the parameters a and b, can quantitatively specify the effect of all the controlling parameters, viz., E_0, ω_0, n_0, and γ_0, on SESR.

The first-order term of our result for the E_ρ component given by Eq. (27) shows consistency with Zachary's [10] result. The term containing the factors $\mp b\epsilon\Omega\omega/c^2$ in Eq. (27) can be identified as the transverse SESR field, viz., E_1 given by Zachary's [10] Eq. (2.13). However, our result shows an additional multiplying factor in E_ρ, viz., $[n_0\sqrt{n_0^2-1}/2(1+\beta_0 n_0)]$, and an additional factor $(2\ \gamma)$ for the shifted frequency Ω. Our result for E_ρ also shows an additional first-order term (not obtained by Zachary) containing the factor $(b/2)$. We attribute this difference to the refinement in calculations introduced by taking the electron's time varying position and energy (rather than their mean values) and using relativistically correct expressions explicitly. Therefore our results are more exact. The first-order term containing b of Eq. (26) also agrees (in magnitude) with the longitudinal SESR field given by Risbud [13], viz., the second term of their Eq. (26). However, as the final expressions specifying the fields of the SESR obtained by Zachary [10] and Risbud [13] are not in closed form [due to unevaluated partial differentials appearing outside the integrals in Eqs. (2.14) and (2.15) of Zachary [10] and Eq. (26) of Risbud [13]] a more exact comparison of the results is not possible. As the results given by Eqs. (26)–(28) are not suitable for numerical estimation of the fields, we have performed the integration with respect to ω and obtained expressions that are suitable for numerical calculation of the field components. This is done in the next section.

IV. NUMERICAL ESTIMATES AND ANALYSIS

Equations (26)–(28) are further written explicitly in terms of ω as

$$E_z(\mathbf{r},t)=\frac{e}{2c^2}\int d\omega\,\omega e^{i\omega t'}\Bigg\{H_0^{(2)}(\rho A)\mu'-H_0^{(2)}(\rho A_\pm)\times\Bigg[\pm\alpha_1\omega\pm\frac{\alpha_2}{\omega}+\alpha_3\Bigg]e^{\mp i4\Omega z/v_0'}+\frac{b}{2}A'_\pm e^{\mp\pi i/2}\times H_0^{(2)}(\rho A'_\pm)\Bigg[\mu'\mp\frac{2\Omega}{\epsilon\beta_0'^2}\frac{1}{\omega}\Bigg]e^{\mp i2\Omega z/v_0'}\Bigg\},\quad(32)$$

$$E_\rho(\mathbf{r},t)=\frac{e}{2\epsilon v_0'}\int d\omega\,e^{i\omega t'}\Bigg\{-AH_0^{(2)}(\rho A)+\frac{A_\pm}{2v_0'}H_0^{(2)}(\rho A_\pm)\times[\pm\alpha_4\omega+\alpha_5]e^{\mp i4\Omega z/v_0'}+\frac{b\epsilon}{2}e^{\mp\pi i/2}H_0^{(2)}(\rho A'_\pm)\times\Bigg[\pm\frac{\Omega}{c^2}\omega+\frac{1}{\epsilon}\Bigg]e^{\mp i2\Omega z/v_0}\Bigg\},\quad(33)$$

and

$$E_\phi(\mathbf{r},t)=\frac{\pi e}{2\epsilon v_0'}\int d\omega\,e^{i\omega t'}\Bigg\{H_0^{(2)}(\rho A)+H_0^{(2)}(\rho A_\pm)\times[\pm\alpha_6\omega+\alpha_7]e^{\mp i4\Omega z/v_0'}+\frac{b}{2}e^{\mp\pi i/2}A'_\pm\times H_0^{(2)}(\rho A'_\pm)e^{\mp i2\Omega z/v_0'}\Bigg\},\quad(34)$$

where

$$t'=t-\frac{z}{v_0'},\quad \mu'=\left(1-\frac{1}{\epsilon\beta_0'^2}\right),\quad \beta_0'=\left|\frac{v_0'}{c}\right|,\quad A^2=a_1\omega^2,$$

$$A_\pm^2=a_1\omega^2\mp b_1\omega-c_1,\quad A_\pm'^2=a_1\omega^2\mp\frac{b_1}{2}\omega-\frac{c_1}{4},$$

$$a_1=\frac{\epsilon\beta_0'^2-1}{v_0'^2},\quad b_1=\frac{8\Omega}{v_0'^2},\quad c_1=\frac{16\Omega}{v_0'^2},$$

$$\alpha_1=\frac{\mu'}{2}\left(\frac{a}{v_0'}-\frac{b^2b_1}{4}\right),$$

$$\alpha_2=\frac{\omega}{\epsilon\beta_0'^2}\left(\frac{b^2c_1}{2}-\frac{8a\Omega}{v_0'}\right),$$

$$\alpha_3=\frac{b^2b_1\Omega}{2\epsilon\beta_0'^2}-\frac{4a\Omega}{v_0'\epsilon\beta_0'^2}-\frac{b^2c_1\mu'}{8},$$

$$\alpha_4=\frac{a}{v_0'}-\frac{b^2b_1}{4}-\frac{b^2\epsilon\Omega}{2c^2},\quad \alpha_5=\frac{4a\Omega}{v_0'}-\frac{b^2c_1}{4},$$

$$\alpha_6=\frac{a}{4v_0'}-\frac{b^2b_1}{8}$$

$$\alpha_7=\frac{a\Omega}{v_0'}-\frac{b^2c_1}{8},\quad \alpha_8=\frac{8b\Omega}{\epsilon\beta_0'^2\sqrt{a_1}}.$$

Note that the first term in E_ϕ given by Eq. (34) containing $H_0^{(2)}(\rho A)$ does not contribute (since its integral can be shown to vanish). In the above equations the second-order terms containing a_1b^2 are not included (since they are quite small). Equations (32)–(34) clearly show that the true SESR contains the frequency components 2Ω and 4Ω, which are upshifted from ω_0, the frequency of the incident electromagnetic wave. Therefore we denote them as SESR-2Ω and SESR-4Ω components. In order to calculate the strength of the SESR fields we further integrate [33] the above equations with respect to ω and obtain the results

$$E_z(\mathbf{r},t)=\frac{-e}{2c^2}\Bigg\{\alpha_9\frac{1}{\sqrt{\rho}L^{3/2}}+\frac{e^{\rho(4\Omega/v_0'\sqrt{\mu'})}}{\rho}\Bigg[\alpha_{10}\cos\left(\frac{4\Omega t'}{\epsilon\beta_0'^2-1}-\frac{4\Omega z}{v_0'}\right)+i\alpha_{11}\sin\left(\frac{4\Omega t'}{\epsilon\beta_0'^2-1}-\frac{4\Omega z}{v_0'}\right)\Bigg]+\frac{e^{\rho(2\Omega/v_0'\sqrt{\mu'})}}{\rho}[\alpha_{13}e^{-i(2\Omega t'/(\epsilon\beta_0'^2-1)-2\Omega z/v_0')}]\Bigg\},\quad(35)$$

$$E_\rho(\mathbf{r},t)=\frac{-e}{2c^2}\Bigg\{\alpha_{14}\frac{1}{\sqrt{\rho}L^{3/2}}+\frac{e^{\rho(4\Omega/v_0'\sqrt{\mu'})}}{\rho}\Bigg[\alpha_{15}\cos\left(\frac{4\Omega t'}{\epsilon\beta_0'^2-1}-\frac{4\Omega z}{v_0'}\right)+i\alpha_{16}\sin\left(\frac{4\Omega t'}{\epsilon\beta_0'^2-1}-\frac{4\Omega z}{v_0'}\right)\Bigg]+\frac{e^{\rho(2\Omega/v_0'\sqrt{\mu'})}}{\rho}\Bigg[\alpha_{17}\cos\left(\frac{2\Omega t'}{\epsilon\beta_0'^2-1}-\frac{2\Omega z}{v_0'}\right)+i\alpha_{18}\sin\left(\frac{2\Omega t'}{\epsilon\beta_0'^2-1}-\frac{2\Omega z}{v_0'}\right)\Bigg]\Bigg\},\quad(36)$$

$$E_\phi(\mathbf{r},t)=\frac{-e}{2c^2}\Bigg\{\frac{e^{\rho(4\Omega/v_0'\sqrt{\mu'})}}{\rho}\Bigg[\alpha_{20}\cos\left(\frac{4\Omega t'}{\epsilon\beta_0'^2-1}-\frac{4\Omega z}{v_0'}\right)+i\alpha_{21}\sin\left(\frac{4\Omega t'}{\epsilon\beta_0'^2-1}-\frac{4\Omega z}{v_0'}\right)\Bigg]+\frac{e^{\rho(2\Omega/v_0'\sqrt{\mu'})}}{\rho}\Bigg[\alpha_{22}\sin\left(\frac{2\Omega t'}{\epsilon\beta_0'^2-1}-\frac{2\Omega z}{v_0'}\right)\Bigg]\Bigg\},\quad(37)$$

where

$$\mathrm{Re}\,L>0,\quad L=t'-\rho\sqrt{a_1},\quad \alpha_9=\frac{\mu'}{4(a_1)^{1/4}},$$

$$\alpha_{10}=\frac{2\alpha_2}{\sqrt{a_1}}+\frac{\alpha_1b_1^2}{2(a_1)^{5/2}},$$

$$\alpha_{11}=\frac{b_1\alpha_3}{(a_1)^{3/2}},\quad \alpha_{13}=\frac{\alpha_8}{2}\left(\frac{b_1^2}{16a_1}+\frac{c_1}{4}\right)^{1/2},$$

$$\alpha_{14}=\frac{ca_1^{1/4}}{4\epsilon\beta_0'},\quad \alpha_{15}=\frac{4\Omega\alpha_5}{\epsilon\beta_0'^2v_0'\sqrt{\mu'}},$$

$$\alpha_{16}=\frac{16\Omega^2\alpha_4}{\epsilon c^2a_1\sqrt{\mu'}},\quad \alpha_{17}=\frac{bc}{\epsilon\beta_0'^2\sqrt{a_1}},\quad \alpha_{18}=\frac{bb_1\Omega}{4v_0'a_1^{3/2}},$$

$$\alpha_{20}=\frac{4\pi\alpha_7}{\epsilon\beta_0'^2\sqrt{a_1}},\quad \alpha_{21}=\frac{2\pi b_1\alpha_6}{\epsilon\beta_0'^2a_1^{3/2}},$$

$$\alpha_{22}=\frac{2\pi b}{\epsilon\beta_0'^2\sqrt{a_1}}\left(\frac{b_1^2}{16a_1}+\frac{c_1}{4}\right)^{1/2}.$$

The compact integrated result specified by Eqs. (35)–(37) is more suitable for numerical estimation of the SESR fields. They also contain all the characteristics of SESR. The first terms of Eqs. (35) and (36) give CR-like fields while all the remaining terms along with those of Eq. (37) give SESR fields in the two modes, viz., 2Ω and 4Ω. The coefficients α_9 and α_{14} specify the amplitudes of CR-like SESR in units of $e/2c^2$. When the external wave is absent, putting $a=0$ in α_9 and α_{14} we recover the corresponding components of the normal CR in units of $e/2c^2$ as

$$\alpha_{12}=\alpha_9|_{a=0}\Rightarrow(E_z)_{\rm CR},\quad \alpha_{19}=\alpha_{14}|_{a=0}\Rightarrow(E_\rho)_{\rm CR}.$$

Both modes of SESR show exponential amplification along ρ and propagation nearly along the z direction. We identify, from the phase factors in the two equations, the components of the propagation vectors of the two modes of SESR as

$$\mathbf{k}_{2\Omega}=\left(\frac{2\Omega}{v_0'\sqrt{\mu'}},\quad 0,\quad \frac{2\Omega\epsilon\beta_0'^2}{v_0'(\epsilon\beta_0'^2-1)}\right)$$

and

$$\mathbf{k}_{4\Omega}=\left(\frac{4\Omega}{v_0'\sqrt{\mu'}},\quad 0,\quad \frac{4\Omega\epsilon\beta_0'^2}{v_0'(\epsilon\beta_0'^2-1)}\right).$$

Hence we find the direction of propagation of both modes with respect to z as the angle θ satisfying the equation

$$\theta=\tan^{-1}\left(\frac{k_\rho}{k_z}\right)=\sin^{-1}\theta_c,$$

where θ_c is the angle of the CR cone.

The above equation is satisfied only for small angles, and so $\theta\leqslant 2^\circ\,10'$. Equations (35)–(37) also show an additional factor $(\epsilon\beta_0'^2-1)^{-1}$ in the frequencies of the two SESR modes. Due to this, the frequency upshift in SESR becomes substantially large [34] as compared to the frequency of the incident electromagnetic wave. The field amplitudes of SESR can be determined by evaluating coefficients $\alpha_9-\alpha_{22}$ when the external parameters E_0, ω_0, γ_0, β_0, and n_0 are specified. In order to study the variation of SESR with respect to external parameters, we have scanned the values in their entire feasible ranges $3\leqslant E_0\leqslant 3\times10^5$ statvolts/cm, $5\times10^7\leqslant\omega_0\leqslant5\times10^{15}$ Hz, and $1.000\,25\leqslant n_0\leqslant 6$.

As $\mu=(\beta_0n_0-1)$, by choosing $10^{-6}\leqslant\mu\leqslant10^{-1}$, we have determined allowed β_0 values for a given n_0 by using $\beta_i<10^{-5}$. The numerical calculations show that as compared to the normal CR the CR-like SESR gives a small reduction, but the true SESR modes (2Ω and 4Ω) show an orders of magnitude increase. As CR is quite weak [15,35] the SESR-2Ω and -4Ω components, even though extremely large as compared to CR, do give feasible values of the fields of a few V/cm. The component E_ϕ given by Eq. (37) is characteristic of SESR (both SESR-2Ω and SESR-4Ω), since CR-like SESR and normal CR do not possess any such ϕ components.

The calculated values of the field components, in the entire range, give the following conclusions. For the CR-like SESR,

$$|E_\rho|>|E_z|,$$

for the SESR-2Ω mode,

$$|(E_\rho)_{2\Omega}|>|(E_z)_{2\Omega}|\gg|(E_\phi)_{2\Omega}|,$$

and for the SESR-4Ω mode,

$$|(E_z)_{4\Omega}|\gg|(E_\rho)_{4\Omega}|\gg|(E_\phi)_{4\Omega}|.$$

Since CR has no E_ϕ component, getting E_ϕ is a field-induced effect. The role of E_ϕ and the source of energy are clear when we calculate Poynting's vector. When the negative sign of the electron is explicitly included and the signs of the appropriate coefficients $(\alpha_9-\alpha_{22})$ are also taken from numerical calculations, different components of the electric field are found to have the following signs. For CR-like SESR, $E_z<0$, $E_\rho>0$, while for SESR-2Ω, $E_z<0$, $E_\rho>0$, $E_\phi>0$, and for SESR-4Ω, $E_z<0$, $E_\rho<0$, $E_\phi<0$.

We calculate the Poynting's vector $\mathbf{S}=(c/4\pi)(\mathbf{E}\times\mathbf{H})$ for SESR, using $\mathbf{H}=(\hat{k}\times\mathbf{E}_0)n_0$, and write its components in units of $cn_0/4\pi$ as follows. For CR-like SESR,

$$(S_\rho)_{\text{CR-like}}>0,\quad (S_z)_{\text{CR-like}}>0.$$

For SESR-2Ω,

$$(S_\rho)_{2\Omega}=-E_\phi^2+E_z(E_\rho-E_z)>0\quad \text{since } |E_\rho|>|E_z|\gg|E_\phi|,$$

$$(S_\phi)_{2\Omega}=E_\phi(E_z+E_\rho)>0,$$

and

$$(S_z)_{2\Omega}=E_\phi^2+E_\rho(E_\rho-E_z)>0\quad \text{since } |E_\rho|>|E_z|.$$

For SESR-4Ω,

TABLE I. Numerical values of the ratios of the field components of $\mathbf{E}_{4\Omega}$ to the corresponding components of $\mathbf{E}_{2\Omega}$ for different sets of external parameters E_0, ω_0, n_0, and β_0.

E_0 (statvolts/cm)	ω_0 (Hz)	n_0	β_0	$(E_\phi)_{4\Omega}/(E_\phi)_{2\Omega}$	$(E_\rho)_{4\Omega}/(E_\rho)_{2\Omega}$	$(E_z)_{4\Omega}/(E_z)_{2\Omega}$
3×10^5	5×10^{15}	1.002 5	0.997 6	3.5×10^{-4}	8.3×10^{-16}	4.98×10^{-4}
3×10^5	5×10^{15}	1.15	0.869 7	2.69×10^{-5}	4.13×10^{-17}	3.68×10^{-5}
3	5×10^{11}	2	0.500 1	4.3×10^{-2}	1.25×10^{-14}	5.7×10^{-2}
3	5×10^{9}	1.000 25	0.999 85	2.2×10^{-4}	5.2×10^{-16}	3.1×10^{-4}

$$(S_\rho)_{4\Omega}=-\{E_\phi^2+E_z(E_\rho+E_z)\}<0,$$

$$(S_\phi)_{4\Omega}=E_\phi(E_\rho-E_z)<0 \quad \text{since } |E_z|\gg|E_\rho|,$$

$$(S_z)_{4\Omega}=E_\phi^2+E_\rho(E_\rho+E_z)>0.$$

We note that the fields of SESR-2Ω are similar in sign to CR-like fields with only the component E_ϕ extra and so its Poynting's vector also has a positive component S_ϕ extra.

Further, as in normal CR, for CR-like SESR S_ρ and S_z are both positive and for SESR-2Ω all three components of $\mathbf{S}$ are positive, while for SESR-4Ω only $(S_z)_{4\Omega}>0$. Therefore we see that CR-like SESR is the same as normal CR with only the amplitude changed. But the SESR-2Ω is different. It gives radiation of upshifted frequency component 2Ω confined to the CR cone, with an additional component of radiation in the ϕ direction. The SESR-4Ω is quite different. It gives radiation of upshifted frequency component 4Ω propagating only in the z direction. Thus we see that due to SESR energy is radiated in the CR cone for SESR-2Ω, and in the (longitudinal) z direction due to SESR-4Ω. So the SESR-4Ω mode is highly directional. The remaining components of the Poynting's vector, which are negative, supply energy to the electron beam. Thus the electron beam absorbs energy from the incident electromagnetic wave and emits it in the form of SESR which is indeed enormously amplified, exponentially growing electromagnetic radiation containing largely upshifted frequency components (as compared to the frequency of the incident electromagnetic wave) 2Ω confined to the CR cone and 4Ω which is highly directional.

From Eqs. (35)–(37) and (26)–(28) it is clear that the first-order effect is given by the terms containing b, while the second-order field effect is shown by the terms containing b^2 and a. In order to separate the second from the first-order effect we put $a=0=b^2$ in Eqs. (35)–(37) and see that obtaining radiation of frequency 2Ω (i.e., SESR-2Ω) is a first-order effect, while getting SESR-4Ω and CR-like SESR are second-order effects. No field effect is just the normal CR. We further find the ratios of the field components for CR-like SESR to be $(E_z)_{\text{CR-like}}/(E_z)_{\text{CR}}\leqslant1$,$(E_\rho)_{\text{CR-like}}/(E_\rho)_{\text{CR}}\leqslant1$, for the entire range of external parameters. For SESR-4Ω and SESR-2Ω we calculate the ratios of the field components for four typical dielectrics (solid, liquid, and gaseous) and show them in Table I.

The numerical values in the Table I clearly show that the second-order field effects are quite small compared to the first-order effects. Therefore, higher order calculations, if performed, may give higher modes like 6Ω, 8Ω, etc., but with rapidly decreasing field amplitudes.

V. GRAPHS AND CONTROLLING PARAMETERS

As the effect of SESR can be observed experimentally and may be of use in obtaining coherent radiation in the frequency region not covered by existing sources, it is of practical importance to study the variation of SESR with different external parameters controlling the effect. Therefore, we have scanned the entire feasible ranges of the parameters where our approximations maybe valid and have calculated the SESR field components. We have considered the values of the parameters in the ranges $3\leqslant E_0\leqslant3\times10^5$ statvolts/cm, $5\times10^7\leqslant\omega_0\leqslant5\times10^{15}$ Hz, and $1.000\,25\leqslant n_0\leqslant6$.

As $\mu=\beta_0 n_0-1$, by choosing $10^{-6}\leqslant\mu\leqslant10^{-1}$, we have determined allowed β_0 values for a given n_0, by using $\beta_i<10^{-5}$. For different sets of values of (β_0, E_0, n_0, and ω_0) we have determined the values of the parameters a and b, evaluated the constants $\alpha_9-\alpha_{22}$, and hence obtained the values of field strengths of SESR components by using Eqs. (35)–(37). Our numerical calculations give the following conclusions.

(1) For any E_0 and n_0 (within the above ranges), there is no effect for $\omega_0\leqslant5\times10^9$ Hz.

(2) For weak fields ($3\leqslant E_0\leqslant300$ statvolts/cm) the effect is possible for all dielectrics (gaseous, solid, and liquid) and for ω_0 lying in the wide range 10^{10}–10^{15} Hz.

(3) For stronger fields ($3\times10^3\leqslant E_0\leqslant3\times10^5$ statvolts/cm) the effect is possible only for gaseous and liquid dielectrics and not for solids, for ω_0 lying in the narrow range 10^{13}–10^{15} Hz.

In Figs. 1–10 we have presented our results graphically. We have expressed all the field components in units of $e/2c^2$, so that a comparison is easy. In Fig. 1 we have shown the correctness of our approximation by plotting the ratios of the important parameters V_i/V_0, β_i, and a/b for different values of μ for $E_0=3$ statvolts/cm, $\omega_0=5\times10^{12}$ Hz, and $n_0=1.544$. In the entire range of μ (i.e., $10^{-2}\leqslant\mu\leqslant10^{-6}$), $V_i/V_0\sim10^{-6}$, $\beta_i\sim10^{-6}$, $a/b\sim10^{-7}$. These values show that we are right in taking a as the second-order parameter and b as the first-order one, while retaining terms linear in a and second order in b and neglecting all higher order terms like ab, a^2, b^3, etc.

β_0 variation

In Figs. 2–4 we have shown the dependence of the electric field components of SESR on the parameter β_0 (which is

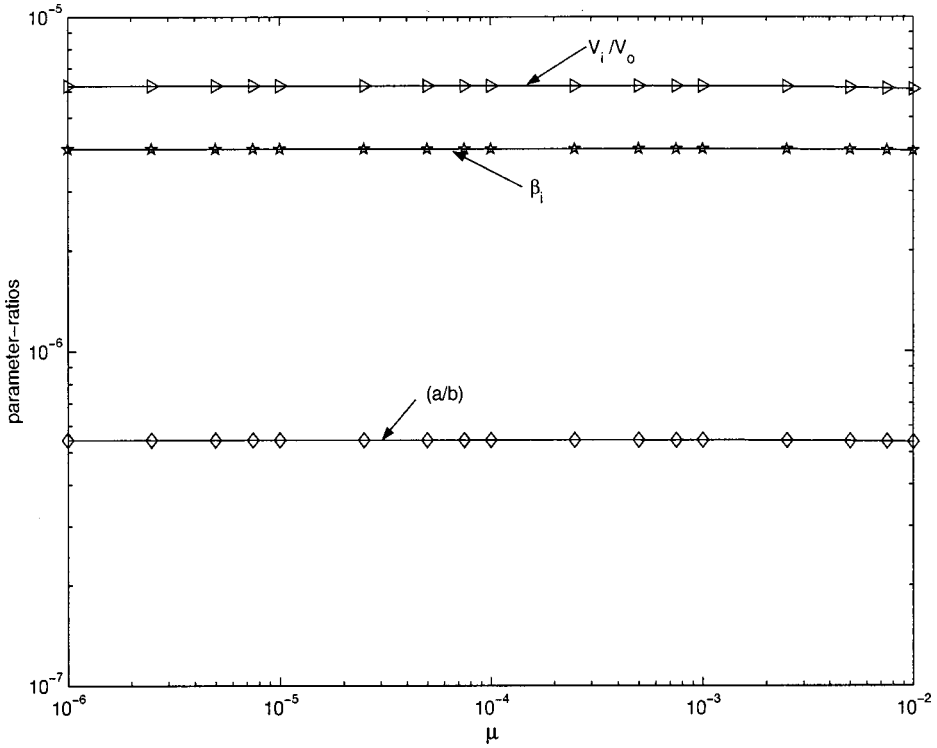

FIG. 1. Variation of the ratios of the parameters V_i/V_0, β_i, and a/b with respect to μ, for $E_0=3$ statvolts/cm, $\omega_0=5\times10^{12}$ Hz, and $n_0=1.544$.

also a measure of the electron energy), for $E_0=3\times10^4$ statvolts/cm, $\omega_0=5\times10^{15}$ Hz, and $n_0=1.0025$. We have shown the variation of the electric field components of CR-like SESR in Fig. 2, SESR-2Ω in Fig. 3, and SESR-4Ω in Fig. 4. Here we need to choose $\beta_0\geqslant0.9975$. Figure 2 shows that $(E_\rho)_{\text{CR-like}}$ always exceeds the corresponding $(E_z)_{\text{CR-like}}$ component. In units of $e/2c^2$, $(E_\rho)_{\text{CR-like}}\sim10^3-10^4$ while $(E_z)_{\text{CR-like}}\sim10^0-10^3$. As β_0 increases the CR-like components increase. The initial increase (when just above the threshold) is faster than the later one.

Figure 3 shows that all three components of $\mathbf{E}_{2\Omega}$ decrease as β_0 increases. Larger values of $\mathbf{E}_{2\Omega}$ can be obtained as we approach nearer to the threshold of superphase motion. In units of $e/2c^2$, $(E_\rho)_{2\Omega}\sim10^{25}-10^{29}$, $(E_z)_{2\Omega}\sim10^{24}-10^{27}$, and $(E_\phi)_{2\Omega}\sim10^7-10^{10}$, showing that $(E_\rho)_{2\Omega}\geqslant(E_z)_{2\Omega}\gg(E_\phi)_{2\Omega}$. Therefore for SESR-2Ω$(E_\phi)_{2\Omega}$ is negligible.

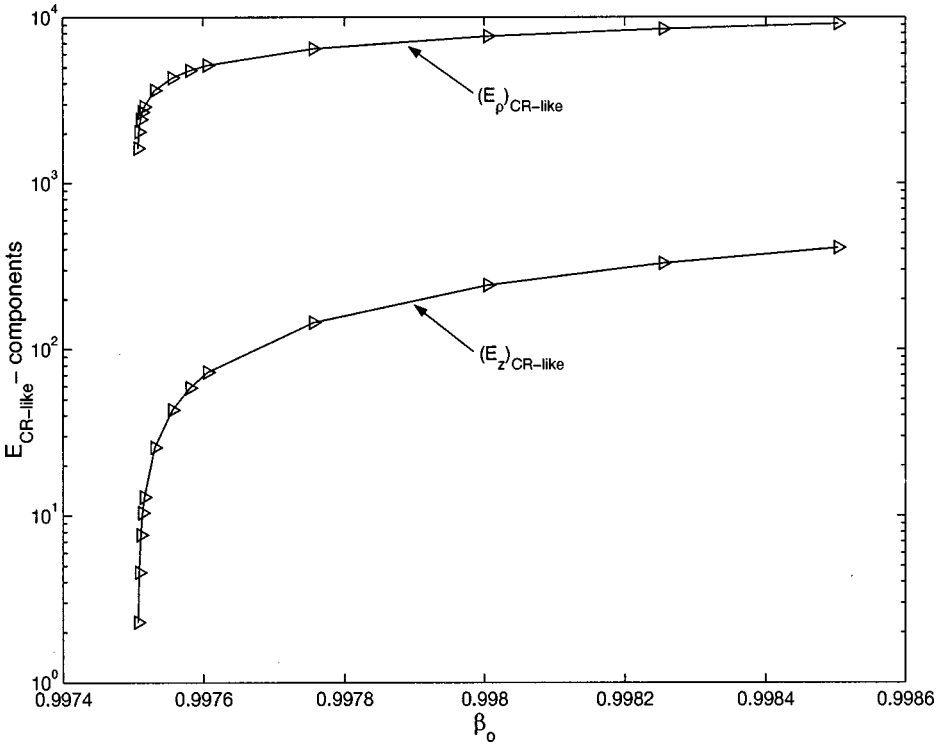

FIG. 2. Componentwise variation of the electric field of CR-like SESR, $\mathbf{E}_{\text{CR-like}}$, in units of $e/2c^2$ with respect to β_0, for $E_0=3\times10^4$ statvolts/cm, $\omega_0=5\times10^{15}$ Hz, and $n_0=1.0025$.

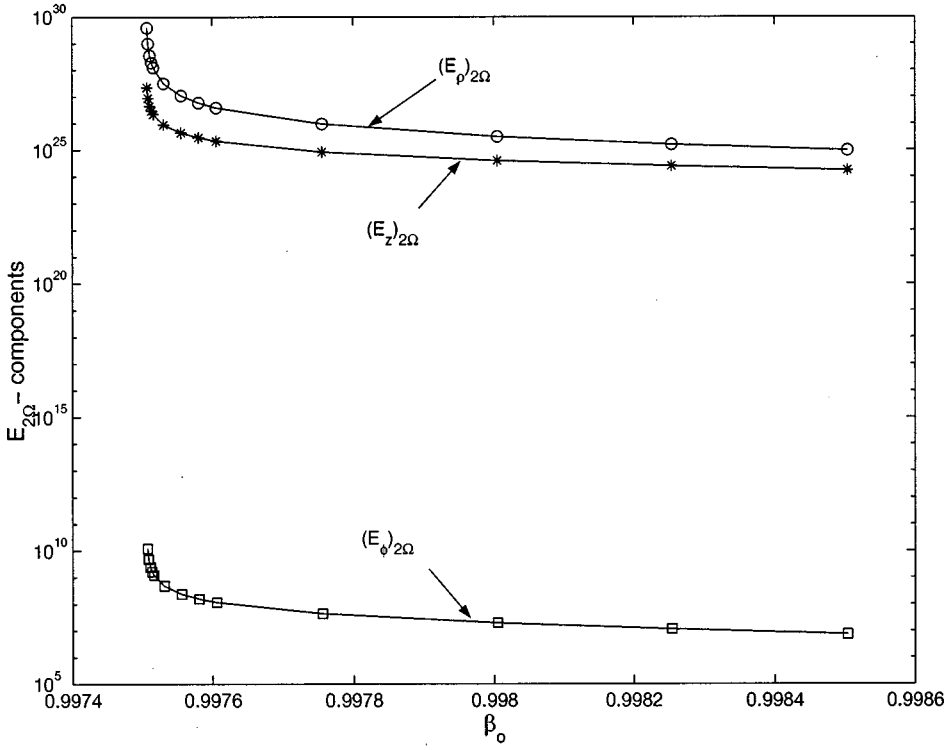

FIG. 3. Componentwise variation of the electric field of SESR-2Ω, $\mathbf{E}_{2\Omega}$, in units of $e/2c^2$ with respect to β_0, for $E_0=3\times10^4$ statvolts/cm, $\omega_0=5\times10^{15}$ Hz, and $n_0=1.0025$.

Figure 4 shows that all three components of $\mathbf{E}_{4\Omega}$ decrease as β_0 increases above threshold. As we approach closer to the threshold value, larger values of $\mathbf{E}_{4\Omega}$ can be obtained. In units of $e/2c^2$,$(E_z)_{4\Omega}\sim10^{19}-10^{24}$, $(E_\rho)_{4\Omega}\sim10^{9}-10^{13}$, and $(E_\phi)_{4\Omega}\sim10^{1}-10^{6}$, showing that $(E_z)_{4\Omega}\gg(E_\rho)_{4\Omega}\gg(E_\phi)_{4\Omega}$. Therefore, for SESR-4Ω only $(E_z)_{4\Omega}$ needs to be considered, while for SESR-2Ω both components $(E_\rho)_{2\Omega}$ and $(E_z)_{2\Omega}$ are important.

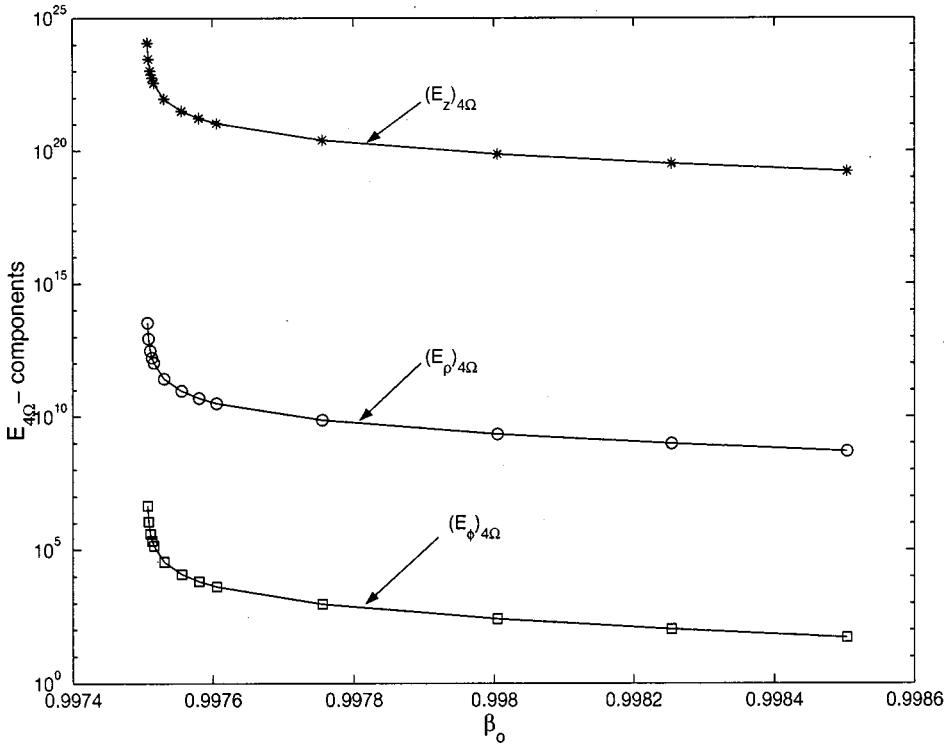

FIG. 4. Componentwise variation of the electric field of SESR-4Ω, $\mathbf{E}_{4\Omega}$, in units of $e/2c^2$ with respect to β_0, for $E_0=3\times10^4$ statvolts/cm, $\omega_0=5\times10^{15}$ Hz, and $n_0=1.0025$.

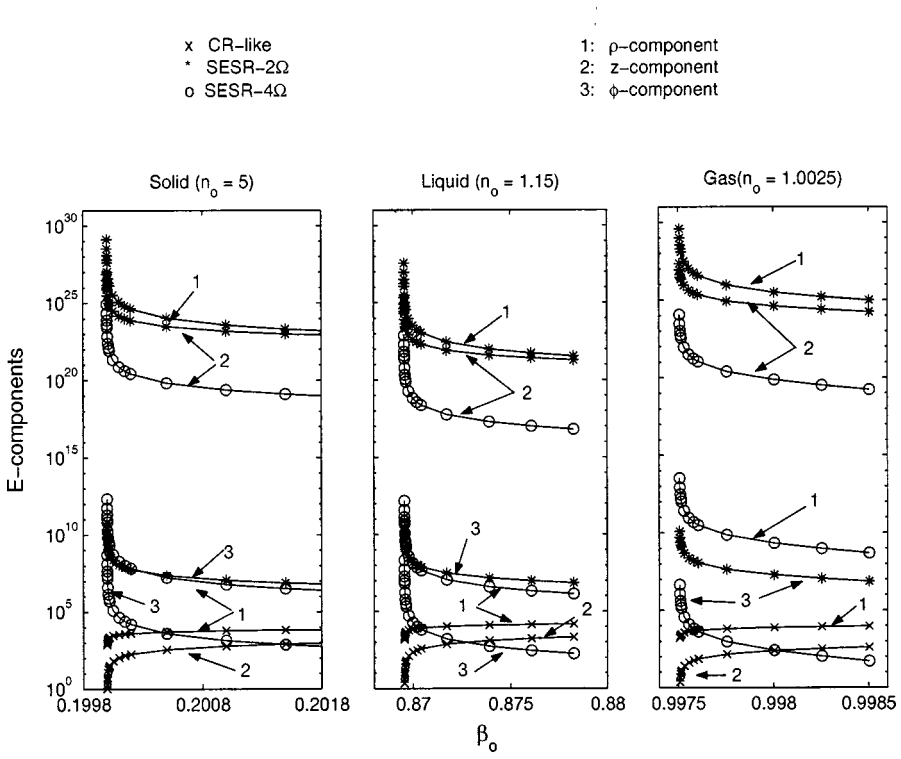

FIG. 5. Componentwise variation of all the electric fields of SESR, $\mathbf{E}_{\text{CR-like}}$, $\mathbf{E}_{2\Omega}$, and $\mathbf{E}_{4\Omega}$, in units of $e/2c^2$ with respect to β_0 (1) for solid with $n_0=5$, $E_0=30$ statvolts/cm, and $\omega_0=5\times10^{15}$ Hz; (2) for liquid with $n_0=1.15$, $E_0=30$ statvolts/cm, and $\omega_0=5\times10^{13}$ Hz; and (3) for gas with $n_0=1.0025$, $E_0=3\times10^4$ statvolts/cm, and $\omega_0=5\times10^{15}$ Hz.

Figures 3 and 4 also show that $(E_z)_{4\Omega}/(E_z)_{2\Omega}\sim10^{-5}-10^{-3}$, $(E_\rho)_{4\Omega}/(E_\rho)_{2\Omega}\sim10^{-16}$, $(E_\phi)_{4\Omega}/(E_\phi)_{2\Omega}\sim10^{-6}-10^{-4}$. Therefore the second-order effect of getting SESR-4Ω is quite small (at least three orders of magnitude less) as compared to the corresponding first-order effect of getting SESR-2Ω.

In Fig. 5 we have shown the variation, at a glance, of all eight components of SESR, viz., $\mathbf{E}_{\text{CR-like}}$, $\mathbf{E}_{2\Omega}$, and $\mathbf{E}_{4\Omega}$, with respect to β_0 for (1) a solid ($n_0=5$) with $E_0=30$ statvolts/cm, $\omega_0=5\times10^{15}$ Hz; (2) a liquid ($n_0=1.15$) with $E_0=30$ statvolts/cm, $\omega_0=5\times10^{13}$ Hz; and (3) a gas ($n_0=1.0025$) with $E_0=10^4$ statvolts/cm, $\omega_0=5\times10^{15}$ Hz. side by side, for easy comparison. All the components appearing in Fig. 5 show behavior similar to that described in Figs. 2–4. Figure 5 shows that for a solid $\beta_0\geqslant0.2$, for a liquid $\beta_0\geqslant0.865$, and for a gas $\beta_0\geqslant0.9975$. Therefore for solids the effect can be obtained for quite small values of β_0 with weak fields (~30 statvolts/cm).

E_0 variation

In Fig. 6 we have shown the componentwise variation of all the electric fields of SESR, viz., $\mathbf{E}_{\text{CR-like}}$, $\mathbf{E}_{2\Omega}$, and $\mathbf{E}_{4\Omega}$, in units of $e/2c^2$ with respect to E_0 in units of statvolts/cm, for $n_0=1.0025$, $\omega_0=5\times10^{15}$ Hz, and $\beta_0=0.9975$. It shows that CR-like SESR is not changed as E_0 is varied. As E_0 is increased $\mathbf{E}_{2\Omega}$ and $\mathbf{E}_{4\Omega}$ also increase but the increase in all the components of $\mathbf{E}_{2\Omega}$ is the same. All the components of $\mathbf{E}_{4\Omega}$ also show the same increase, but the increase of the components of $\mathbf{E}_{4\Omega}$ is more than for those of $\mathbf{E}_{2\Omega}$. This is quite right since getting $\mathbf{E}_{4\Omega}$ is a second-order field effect while getting $\mathbf{E}_{2\Omega}$ is a first-order one.

ω_0 variation

In Fig. 7 we have shown the componentwise variation of all the electric fields of SESR, viz., $\mathbf{E}_{\text{CR-like}}$, $\mathbf{E}_{2\Omega}$, and $\mathbf{E}_{4\Omega}$, in units of $e/2c^2$ with respect to ω_0 in Hz, for $E_0=3$ statvolts/cm, $n_0=1.025$, and $\beta_0=0.9854$. It shows that there is no change in CR-like SESR as ω_0 is varied. The ρ and z components of SESR-2Ω remain the same while its ϕ component decreases. But all the components of $\mathbf{E}_{4\Omega}$ show a linear decrease as ω_0 is increased. Thus as we go from the optical to the microwave region SESR-2Ω remains unchanged, but SESR-4Ω gives a greater contribution in the microwave region than in the optical region.

n_0 variation

In Fig. 8 we have shown the componentwise variation of the electric field of SESR, viz., $\mathbf{E}_{\text{CR-like}}$, $\mathbf{E}_{2\Omega}$, and $\mathbf{E}_{4\Omega}$ in units of $e/2c^2$ with respect to n_0, for $E_0=3$ statvolts/cm, $\omega_0=5\times10^{13}$ Hz, and $\mu=5\times10^{-5}$. CR-like SESR shows a very small linear reduction while all other components show an increase with increase in n_0. SESR-2Ω and SESR-4Ω show a very fast rise in the field components up to $n_0\leqslant1.2$. For larger values of n_0 the increase in the field components is slower.

In Fig. 9 we have shown the variation of the ratios of the electric field components of $\mathbf{E}_{4\Omega}$ to the corresponding components of $\mathbf{E}_{2\Omega}$ with respect to μ, for $E_0=3$ statvolts/cm, $\omega_0=5\times10^{12}$ Hz, and $n_0=1.544$. It shows that $(E_\rho)_{4\Omega}/(E_\rho)_{2\Omega}\sim10^{-15}$, $(E_z)_{4\Omega}/(E_z)_{2\Omega}\sim10^{-2}$, and $(E_\phi)_{4\Omega}/(E_\phi)_{2\Omega}\sim10^{-2}-10^{-3}$. Therefore we can say that the first-order effect of getting SESR-2Ω dominates over the

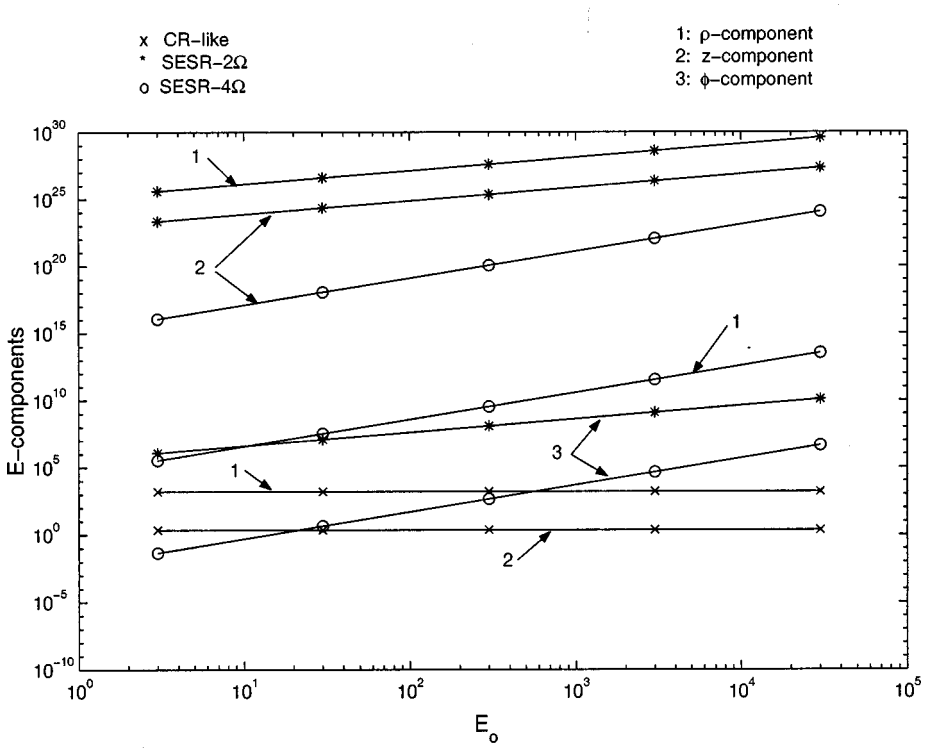

FIG. 6. Componentwise variation of all the electric fields of SESR, $\mathbf{E}_{\text{CR-like}}$, $\mathbf{E}_{2\Omega}$, and $\mathbf{E}_{4\Omega}$, in units of $e/2c^2$ with respect to E_0 in units of statvolts/cm, for $n_0=1.0025$, $\omega_0=5\times10^{15}$ Hz, and $\beta_0=0.9975$.

second-order effect of getting SESR-4Ω.

In Fig. 10 we have shown the variation of CR-like SESR with respect to β_0. To compare it with the normal CR we have expressed the CR-like SESR components in units of the corresponding CR components. Figure 10 also shows that $(E_\rho)_{\text{CR-like}}/(E_\rho)_{\text{CR}}\leqslant 1$ and $(E_z)_{\text{CR-likes}}/(E_z)_{\text{CR}}\leqslant 1$. Therefore CR-like SESR never exceeds the corresponding normal CR. Very near to the threshold ($0.1666<\beta_0<0.1668$) there is a maximum reduction in CR-like SESR, which is ~0.12%. Thus normal CR is almost unaffected.

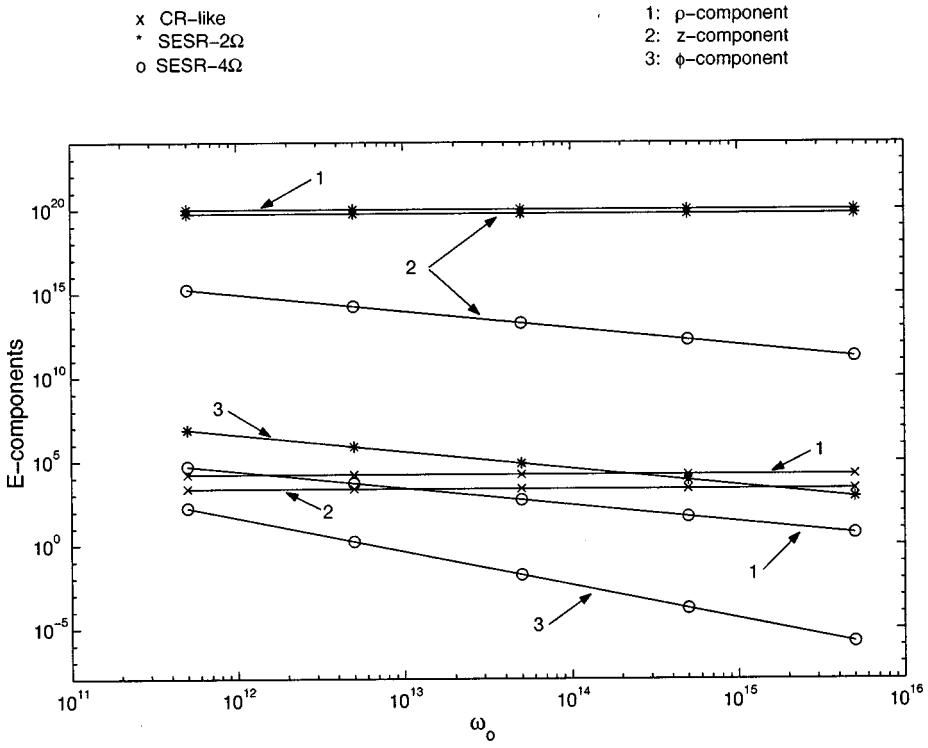

FIG. 7. Componentwise variation of all the electric fields of SESR, $\mathbf{E}_{\text{CR-like}}$, $\mathbf{E}_{2\Omega}$, and $\mathbf{E}_{4\Omega}$, in units of $e/2c^2$ with respect to ω_0 in Hz, for $E_0=3$ statvolts/cm, $n_0=1.025$, and $\beta_0=0.9854$.

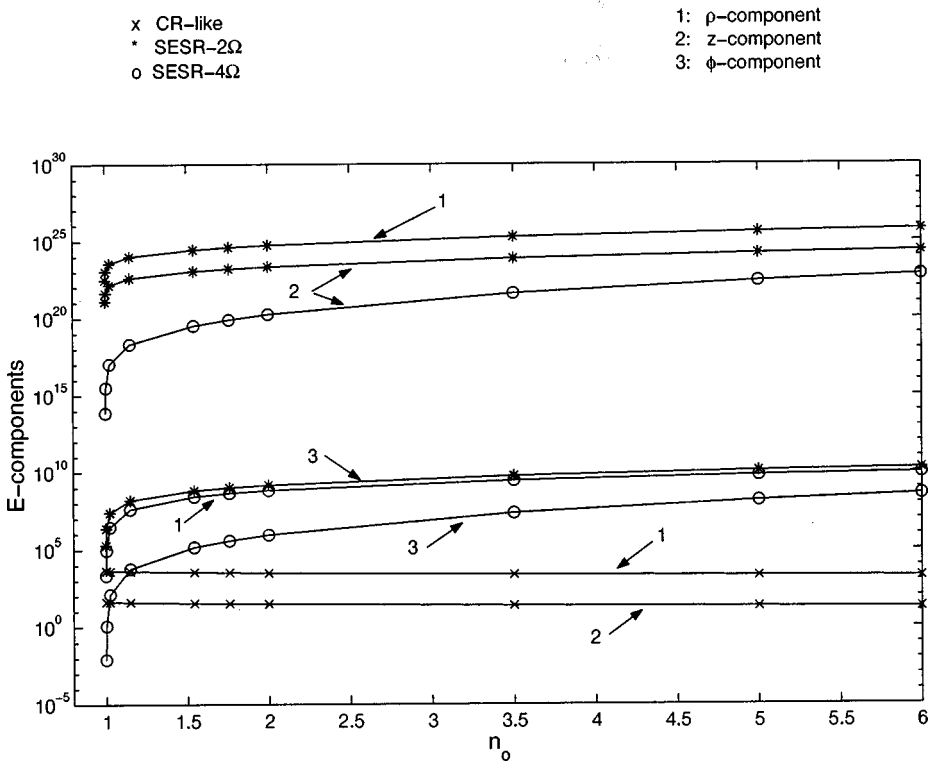

FIG. 8. Componentwise variation of all the electric fields of SESR, $\mathbf{E}_{\text{CR-like}}$, $\mathbf{E}_{2\Omega}$, and $\mathbf{E}_{4\Omega}$, in units of $e/2c^2$ with respect to n_0, for $E_0=3$ statvolts/cm, $\omega_0=5\times10^{13}$ Hz, and $\mu=5\times10^{-5}$.

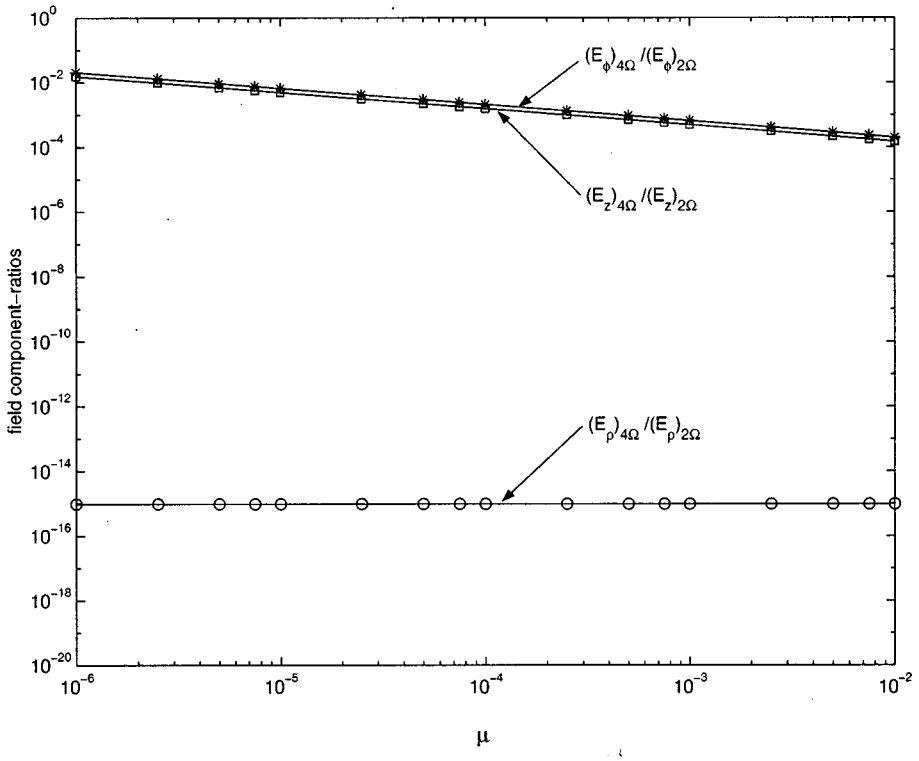

FIG. 9. Variation of the ratios of the electric field components of $\mathbf{E}_{4\Omega}$ to the corresponding components of $\mathbf{E}_{2\Omega}$ with respect to μ for $E_0=3$ statvolts/cm, $\omega_0=5\times10^{12}$ Hz, and $n_0=1.544$.

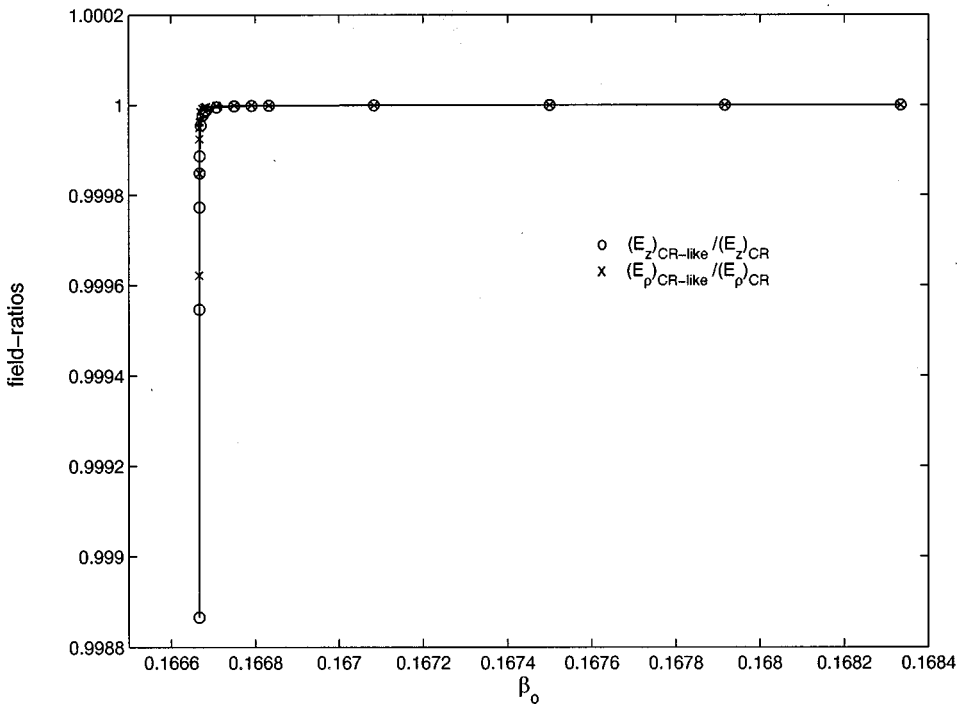

FIG. 10. Variation of the ratios of the electric field components $(E_\rho)_{\text{CR-like}}/(E_\rho)_{\text{CR}}$ and $(E_z)_{\text{CR-like}}/(E_z)_{\text{CR}}$ with respect to β_0, for $E_0=300$ statvolts/cm, $\omega_0=5\times10^{15}$ Hz, and $n_0=6$.

VI. SUMMARY AND CONCLUSIONS

Summary

Our rigorous classical relativistic second-order calculations have shown that SESR indeed gives out exponentially growing, highly directional, enormously amplified electromagnetic radiation of greatly upshifted frequency components viz., 2Ω and 4Ω (where $10^1\leqslant\Omega/\omega_0\leqslant10^7$), propagating nearly along the z direction (within the cone of angle $\theta<2^\circ\,10'$). The 2Ω component is due to the first-order field effect and the 4Ω is because of the second-order field effect. The 4Ω component is much smaller in amplitude (by at least two orders of magnitude) than the 2Ω component. Therefore, if higher order calculations are performed, we expect to obtain higher frequency modes with successively rapidly decreasing amplitudes, i.e., the third-order effect may give a 6Ω component, fourth-order may give an 8Ω component, and so on, but their amplitudes will be successively smaller. As the second-order calculation was quite involved, in order to check whether or not it gave any interesting results the simplest situation of a dispersionless dielectric was chosen. It indeed resulted in the following interesting conclusions.

Conclusions

(1) In the regime of small fields, our rigorous calculations do confirm most of the claims made by Schneider and Spitzer [1–6] in the case of a nondispersive dielectric medium.

(2) Our final expressions [Eqs. (35)–(37)] do show all the characteristics of SESR, namely, directionality, coherence, orders of magnitude enhancement over ordinary CR, exponential growth, and a large upshift in frequency as compared to the incident electromagnetic wave in the most sensitive region, which is just above (i.e., very much in the vicinity of) the threshold of superphase motion.

(3) Our results can provide the field strengths of SESR exactly.

(4) Our graphical results provide the variation of SESR with respect to all the external parameters β_0, E_0, ω_0, and n_0 governing the process and hence can be used for their selection to perform experiments.

(5) The results obtained are of importance in achieving a tunable source of coherent radiation in the frequency region not covered by existing sources.

Since these second-order calculations have revealed many interesting and useful results, further calculations for the dispersive dielectrics are necessary for more realistic situations. Strictly speaking, the assumption that the electron's velocity is constant is not true. Because of unwanted processes like scattering, excitation, ionization, etc., the electron loses energy and does not remain for a long time in phase with the wave. In order to minimize these losses, the electron can be passed parallel to but just above the surface of a dielectric and so the situation of a semi-infinite dielectric may be of practical importance. Work in this direction is in progress and results will be communicated elsewhere.

ACKNOWLEDGMENTS

The authors are thankful to Professor S. V. Lavande, Professor Y. R. Waghmare, and Dr. A. D. Gangal for helpful discussions, Dr. S. B. Sane and Mridula Chandola for technical support, and the Department of Science and Technology (DST), India, for financial support.

APPENDIX A

Substituting from Eqs. (6)–(9) in Eq. (5) and writing the resulting equations componentwise we get [36]

$$F_x = 0, \tag{A1}$$

$$F_y = -eE_i\gamma\epsilon\left(1+\frac{n_0 v_z}{c}\right) = \frac{d}{dt}(\gamma m_0 v_y), \tag{A2}$$

$$F_z = \frac{e\gamma\epsilon}{c}E_i n_0 v_y = \frac{d}{dt}(\gamma m_0 v_z). \tag{A3}$$

Substituting for the velocity components using Eq. (10) and keeping only the first-order terms in μ [37] we get

$$\gamma = \frac{n_0}{\sqrt{n_0^2-1}}\left[1+\frac{\mu u_z}{n_0^2-1}\right]. \tag{A4}$$

Using Eqs. (10) and (A4) in Eqs. (A2) and (A3), keeping only the dominant first-order terms in μ, we get

$$\frac{du_y}{dt} = -\frac{d}{\mu}\sin(\phi_0+2\Omega t), \tag{A5}$$

$$\frac{du_z}{dt} = f u_y \sin(\phi_0+2\Omega t), \tag{A6}$$

where

$$f = \frac{eE_0\gamma(n_0^2-1)^{3/2}}{m_0 c}, \quad d = \frac{2e\gamma\epsilon E_0\sqrt{n_0^2-1}}{m_0 c},$$

and the initial phase $\phi_0 = k_0 z_0$.

Integrating Eqs. (A5) and (A6) with respect to t and using the initial conditions [38] we get

$$u_y = \frac{-d}{2\mu\Omega}\sin 2\Omega t, \tag{A7}$$

$$u_z = 1+\frac{fd}{16\mu\Omega^2}(\cos 4\Omega t - 1). \tag{A8}$$

Substituting Eqs. (A7) and (A8) in Eqs. (10),

$$v_y = -\frac{cd}{2\Omega n_0}\sin 2\Omega t, \tag{A9}$$

$$v_z = v_0 + v_z', \tag{A10}$$

where $v_0 = (c/n_0)(1+\mu)$ and $v_z' = (cfd/16\Omega^2 n_0)(\cos 4\Omega t - 1)$.

APPENDIX B

E_z component

To calculate the E_z component from Eq. (25a) we use the relation (25b) and combine the j_0 part of the j_z term [given by Eqs. (22) and (23)] with the $k_z\rho$ term, and calculate the j_1 part of the j_z term [given by Eqs. (22) and (24)] separately. Substituting the value of $\rho(\mathbf{k},\omega)$ from Eq. (20) and j_1 from Eq. (24) in Eq. (25a) we write the E_z component as

$$(E_z) = (E_z)_1 + (E_z)_2, \tag{B1}$$

where

$$(E_z)_1 = \frac{-iev_0'}{2\pi^2 c^2}\sum_{l,m=-\infty}^{+\infty} e^{l\pi i/2} \times \int_0^\infty k_\rho dk_\rho \int_0^{2\pi} d\phi \int_{-\infty}^{+\infty} dk_z \int_{-\infty}^{+\infty} d\omega \times e^{i[\omega t - k_\rho\rho\cos(\phi-\phi') - k_z z]} J_l(bk_\rho) J_m(ak_z) \times \delta(\omega - k_z v_0' - 2\Omega(l+2m))\frac{1-c^2k_z/v_0'\epsilon\omega}{-k_\rho^2-k_z^2+\epsilon\omega^2/c^2} \tag{B2}$$

and

$$(E_z)_2 = \frac{-iea\Omega}{\pi^2 c^2}\sum_{l,m=-\infty}^{+\infty} e^{l\pi i/2} \times \int_0^\infty k_\rho dk_\rho \int_0^{2\pi} d\phi \int_{-\infty}^{+\infty} dk_z \int_{-\infty}^{+\infty} d\omega\,\omega \times e^{i(\omega t - k_\rho\rho\cos(\phi-\phi') - k_z z)}\left(\frac{J_l(bk_\rho)J_m(ak_z)}{k_\rho^2+k_z^2-\epsilon\omega^2/c^2}\right) \times [\delta(\omega - k_z v_0' - 2\Omega(l+2m+2)) + \delta(\omega - k_z v_0' - 2\Omega(l+2m-2))]. \tag{B3}$$

To perform the multiple integrals appearing in Eqs. (B2) and (B3) we evaluate first the integral with respect to ϕ as [5]

$$\int_0^{2\pi} d\phi\, e^{-ik_\rho\rho\cos(\phi-\phi')} = 2\pi J_0(\rho k_\rho), \tag{B4}$$

and then do the integrals with respect to k_z using the properties of the δ function (which imply that the integrands will contribute only for particular values of k_z specified by the arguments of the δ functions appearing therein). The integrals with respect to k_ρ performed last [39] are found to be of the type [40]

$$\int_0^\infty \frac{k_\rho dk_\rho J_0(\rho k_\rho) J_n(bk_\rho)}{k_\rho^2 - B^2} \propto H_0^{(2)}(\rho B) J_n(bB), \quad \mathrm{Re}\, B > 0, \tag{B5}$$

where $n = 0,1,2,\ldots$ and $H_0^{(2)}(\rho B)$ is the Hankel function of the second kind. In the present second-order calculations, we neglect higher order terms in $a^2, a^3, \ldots$ and $b^3, b^4, \ldots$ while

retaining terms containing a, b, and b^2 in the integrated expressions derived from Eqs. (B2) and (B3) by using Eqs. (B4) and (B5). As $J_l(bB)\propto(bB)^l/l!$, it is enough to take the contributions from $l=0,\pm1,\pm2$ and $m=0,\pm1$ terms out of infinite sums with respect to l and m appearing in Eqs. (B2) and (B3). Thus after performing the multiple integrals appearing in Eqs. (B2) and (B3) and summing with respect to l in the integrated expressions we get

$$
\begin{aligned}
(E_z)_1=\frac{e}{2c^2}\sum_{m=0,\pm1}\int \omega\, d\omega\, e^{i\omega t}\Bigg\{&\left(1-\frac{c^2k_0}{v_0'\epsilon\omega}\right)J_m(ak_0)J_0(bA_0)H_0^{(2)}(\rho A_0)e^{-ik_0z}-\left(1-\frac{c^2k_{+2}}{v_0'\epsilon\omega}\right)J_m(ak_{+2})J_2(bA_{+2})\\
&\times H_0^{(2)}(\rho A_{+2})e^{-ik_{+2}z}-\left(1-\frac{c^2k_{-2}}{v_0'\epsilon\omega}\right)J_m(ak_{-2})J_2(bA_{-2})H_0^{(2)}(\rho A_{-2})e^{-ik_{-2}z}\\
&+e^{-\pi i/2}\Bigg[\left(1-\frac{c^2k_{+1}}{v_0'\epsilon\omega}\right)J_m(ak_{+1})J_1(bA_{+1})H_0^{(2)}(\rho A_{+1})e^{-ik_{+1}z}+\left(1-\frac{c^2k_{-1}}{v_0'\epsilon\omega}\right)J_m(ak_{-1})J_1(bA_{-1})\\
&\times H_0^{(2)}(\rho A_{-1})e^{-ik_{-1}z}\Bigg]\Bigg\}
\end{aligned}
\tag{B6}
$$

and

$$
\begin{aligned}
(E_z)_2=\frac{ea\Omega}{c^2v_0'}\sum_{m=0,\pm1}\int \omega\, d\omega\, e^{i\omega t}\{&J_m(ak_{+2})J_0(bA_{+2})H_0^{(2)}(\rho A_{+2})e^{-ik_{+2}z}+J_m(ak_{-2})J_0(bA_{-2})H_0^{(2)}(\rho A_{-2})e^{-ik_{-2}z}\\
&-J_m(ak'_{+2})J_2(bA'_{+2})H_0^{(2)}(\rho A'_{+2})e^{-ik'_{+2}z}-2J_m(ak_0)J_2(bA_0)H_0^{(2)}(\rho A_0)e^{-ik_0z}-J_m(ak'_{-2})J_2(bA'_{-2})\\
&\times H_0^{(2)}(\rho A'_{-2})e^{-ik'_{-2}z}+e^{-\pi i/2}[J_m(ak'_{+1})J_1(bA'_{+1})H_0^{(2)}(\rho A'_{+1})e^{-ik'_{+1}z}+J_m(ak_{-1})J_1(bA_{-1})H_0^{(2)}(\rho A_{-1})e^{-ik_{-1}z}\\
&+J_m(ak_{+1})J_1(bA_{+1})H_0^{(2)}(\rho A_{+1})e^{-ik_{+1}z}+J_m(ak'_{-1})J_1(bA'_{-1})H_0^{(2)}(\rho A'_{-1})e^{-ik'_{-1}z}]\},
\end{aligned}
\tag{B7}
$$

where

$$
\begin{aligned}
k_0&=\frac{\omega-4m\Omega}{v_0'},\quad A_0^2=\frac{\epsilon\omega^2}{c^2}-k_0^2,\\
k_{\pm1}&=\frac{\omega-4m\Omega\mp2\Omega}{v_0'},\quad A_{\pm1}^2=\frac{\epsilon\omega^2}{c^2}-k_{\pm1}^2,\\
k_{\pm2}&=\frac{\omega-4m\Omega\mp4\Omega}{v_0'},\quad A_{\pm2}^2=\frac{\epsilon\omega^2}{c^2}-k_{\pm2}^2,\\
k'_{\pm1}&=\frac{\omega-4m\Omega\mp6\Omega}{v_0'},\quad A'^2_{\pm1}=\frac{\epsilon\omega^2}{c^2}-k'^2_{\pm1},\\
k'_{\pm2}&=\frac{\omega-4m\Omega\mp8\Omega}{v_0'},\quad A'^2_{\pm2}=\frac{\epsilon\omega^2}{c^2}-k'^2_{\pm2}.
\end{aligned}
$$

Comparing term by term and appropriately combining Eqs. (B6) and (B7) and rearranging we get from Eq. (B1) the following equation for the E_z component:

$$
\begin{aligned}
E_z(\mathbf{r},t)=\frac{e}{2c^2}\sum_{m=0,\pm1}\int \omega\, d\omega\, e^{i\omega t}\Bigg(&J_m(ak_0)H_0^{(2)}(\rho A_0)\left[\left(1-\frac{c^2k_0}{v_0'\epsilon\omega}\right)J_0(bA_0)-\frac{4a\Omega}{v_0'}J_2(bA_0)\right]\\
&\times e^{-ik_0z}+J_m(ak_{+2})H_0^{(2)}(\rho A_{+2})\left[-\left(1-\frac{c^2k_{+2}}{v_0'\epsilon\omega}\right)J_2(bA_{+2})+\frac{2a\Omega}{v_0'}J_0(bA_{+2})\right]e^{-ik_{+2}z}+J_m(ak_{-2})H_0^{(2)}(\rho A_{-2})\\
&\times\left[-\left(1-\frac{c^2k_{-2}}{v_0'\epsilon\omega}\right)J_2(bA_{-2})+\frac{2a\Omega}{v_0'}J_0(bA_{-2})\right]e^{-ik_{-2}z}-\frac{2a\Omega}{v_0'}[J_m(ak'_{+2})J_2(bA'_{+2})H_0^{(2)}(\rho A'_{+2})e^{-ik'_{+2}z}
\end{aligned}
$$

$$+J_m(ak'_{-2})J_2(bA'_{-2})H_0^{(2)}(\rho A'_{-2})e^{-ik'_{-2}z}]+e^{-(\pi i/2)}\Bigg\{J_m(ak_{+1})H_0^{(2)}(\rho A_{+1})J_1(bA_{+1})\left[\frac{2a\Omega}{v'_0}+\left(1-\frac{c^2k_{+1}}{v'_0\epsilon\omega}\right)\right]$$

$$\times e^{-ik_{+1}z}+J_m(ak_{-1})H_0^{(2)}(\rho A_{-1})J_1(bA_{-1})\left[\frac{2a\Omega}{v'_0}+\left(1-\frac{c^2k_{-1}}{v'_0\epsilon\omega}\right)\right]e^{-ik_{-1}z}+\frac{2a\Omega}{v'_0}J_m(ak'_{+1})$$

$$\times H_0^{(2)}(\rho A'_{+1})J_1(bA'_{+1})e^{-ik'_{+1}z}+\frac{2a\Omega}{v'_0}J_m(ak'_{-1})H_0^{(2)}(\rho A'_{-1})J_1(bA'_{-1})e^{-ik'_{-1}z}\Bigg\}\Bigg). \tag{B8}$$

We calculate the $m=0$ and $m=\pm 1$ contributions separately from Eq. (B8) using

$$J_0(ak_0)\sim 1, \quad J_1(ak)\sim\frac{ak}{2},$$

$$J_0(bA)\sim\left(1-\frac{b^2A^2}{4}\right), \quad J_2(bA)\sim\frac{(bA)^2}{8}.$$

Keeping terms linear in b and a and second order in b while neglecting terms of the order of ab and then comparing and appropriately combining the terms in Eq. (B8), we finally get Eq. (26) for the E_z component.

E_ρ component

To calculate the E_ρ component we use the relation (25c) and substitute the values of $j_\rho(\mathbf{k},\omega)$ from Eq. (21) and $\rho(\mathbf{k},\omega)$ from Eq. (20) in Eq. (25a) to obtain

$$E_\rho=(E_\rho)_1+(E_\rho)_2, \tag{B9}$$

where

$$(E_\rho)_1=\frac{-ieb\Omega}{4\pi^2c^2}\sum_{l,m=-\infty}^{+\infty}e^{(i\pi/2)(l-1)}$$

$$\times\int_0^\infty k_\rho dk_\rho\int_0^{2\pi}d\phi\int_{-\infty}^{+\infty}dk_z\int_{-\infty}^{+\infty}\omega\,d\omega$$

$$\times e^{i[\omega t-k_\rho\rho\cos(\phi-\phi')-k_zz]}\frac{J_l(bk_\rho)J_m(ak_z)}{k_\rho^2+k_z^2-\epsilon\omega^2/c^2}$$

$$\times\{\delta(\omega-k_zv'_0-2\Omega(l+2m+1))$$

$$-\delta(\omega-k_zv'_0-2\Omega(l+2m-1))\} \tag{B10}$$

and

$$(E_\rho)_2=\frac{-ie}{\pi\epsilon}\sum_{l,m=-\infty}^{+\infty}e^{i\pi l/2}\int_0^\infty k_\rho^2dk_\rho\int_0^{2\pi}d\phi\int_{-\infty}^{+\infty}dk_z\int_{-\infty}^{+\infty}d\omega$$

$$\times e^{i[\omega t-k_\rho\rho\cos(\phi-\phi')-k_zz]}\frac{J_l(bk_\rho)J_m(ak_z)}{k_\rho^2+k_z^2-\epsilon\omega^2/c^2}$$

$$\times[\delta(\omega-k_zv'_0-2\Omega(l+2m))]. \tag{B11}$$

From Eqs. (B10) and (B11) we observe that the ϕ integral appearing in this case is the same as that given by Eq. (B4). The integral with respect to k_z can be performed using δ functions. The k_ρ integrals appearing in Eq. (B10) are again of the same type given by Eq. (B5) while that appearing in Eq. (B11) is different, containing k_ρ^2 (rather than k_ρ), but can be evaluated [39] to get Eq. (27) for E_ρ.

E_ϕ component

To calculate the E_ϕ component from Eq. (25a) we use the relation (25d), substitute the value of $\rho(\mathbf{k},\omega)$ from Eq. (20), and obtain

$$E_\phi(\mathbf{r},t)=\frac{-ie}{2\pi^2\epsilon}\sum_{l,m=-\infty}^{+\infty}e^{i\pi l/2}$$

$$\times\int_0^\infty k_\rho dk_\rho\int_0^{2\pi}d\phi\,\phi\int_{-\infty}^{+\infty}dk_z\int_{-\infty}^{+\infty}d\omega$$

$$\times e^{i[\omega t-k_\rho\rho\cos(\phi-\phi')-k_zz]}\frac{J_l(bk_\rho)J_m(ak_z)}{k_\rho^2+k_z^2-\epsilon\omega^2/c^2}$$

$$\times[\delta(\omega-k_zv'_0-2\Omega(l+2m))]. \tag{B12}$$

We first evaluate the integral with respect to k_z using the δ function. We observe that in this case the integral with respect to ϕ is changed. Denoting it by I_ϕ we write from Eq. (B12)

$$I_\phi=\int_0^{2\pi}\phi e^{ik_\rho\rho\cos(\phi-\phi')}d\phi. \tag{B13}$$

To evaluate I_ϕ we use Eq. (19) to express the exponential in terms of the Bessel function $J_n(k_\rho\rho)$ (which, being independent of ϕ, can be taken outside the integral with respect to ϕ) and obtain

$$I_\phi=\sum_{n=-\infty}^{+\infty}(-i)^nJ_n(k_\rho\rho)e^{-in\phi'}I'_\phi, \tag{B14}$$

where

$$I'_\phi=\int_0^{2\pi}\phi e^{-in\phi'}d\phi,$$

which is evaluated for the $n\neq 0$ and $n=0$ cases separately to obtain

$$I'_{\phi}=\begin{cases}\dfrac{2\pi}{-in} & \text{for } n\neq 0\\ 2\pi^2 & \text{for } n=0.\end{cases} \tag{B15}$$

The integral with respect to k_ρ appearing in Eq. (B12) is of the same type given by Eq. (B5). Performing the multiple integrals appearing in Eq. (B12) with the help of Eqs. (B5), (B13), (B14), and (B15) and retaining terms up to second order [41], and properly simplifying, we obtain the E_ϕ component as given by Eq. (28).

APPENDIX C

For integrating Eqs. (32)–(34) with respect to ω, we use the asymptotic form of $H_0^{(2)}(\rho A)$, viz.,

$$H_0^{(2)}(\rho A)\rightarrow\sqrt{2/\pi\rho A}e^{-i\rho A}e^{\pi i/4}. \tag{C1}$$

The first (CR-like) terms of Eqs. (32) and (33) can be integrated using tables [30] to give

$$\int_{-\infty}^{+\infty}\sqrt{\omega}\,d\omega\,e^{i\omega L}=-\frac{\sqrt{\pi}}{2\sqrt{2}}\frac{1}{L^{3/2}},\quad \mathrm{Re}\,L>0. \tag{C2}$$

The remaining SESR terms of Eqs. (32)–(34) can be integrated using the well known approximation formula [29] given by the stationary phase method [24] as

$$\int_{\omega_1}^{\omega_2}d\omega\,\Phi(\omega)e^{if(\omega)}=\frac{\sqrt{2\pi}\Phi(\omega_0')}{\sqrt{|f''(\omega_0')|}}e^{if(\omega_0')\pm i\pi/4}, \tag{C3}$$

where ω_0' denotes the root of the equation

$$f'(\omega_0')=\left.\frac{df}{d\omega}\right|_{\omega=\omega_0'}=0, \tag{C4}$$

which lies within the range of the integration ($\omega_1<\omega_0'<\omega_2$), and where the upper or the lower sign is to be taken in the exponential as $f''(\omega_0')$ is positive or negative.

If Eq. (C4) has no roots within the range of integration, the integral (C3) vanishes in the first approximation. Equation (C3) is valid under the condition that $e^{if(\omega)}$ goes through a large number of periods within the range of integration, while $\Phi(\omega)$ changes comparatively slowly and the value of $f'''(\omega_0')\{f''(\omega_0')\}^{-3/2}$ is small.

We convert the integrals appearing in Eqs. (32)–(34) from $(-\infty,+\infty)$ to $(0,\infty)$, combine the $A_\pm$ and $A'_\pm$ terms appropriately, and use Eq. (C3) to obtain the integrals

$$\int_{-\infty}^{+\infty}d\omega\,e^{i\omega t'}H_0^{(2)}(\rho A_\pm)e^{\mp i(4\Omega z/v_0')}=\frac{4}{\sqrt{i}\sqrt{a_1}}\frac{e^{\rho\sqrt{b_1^2/4a_1+c_1}}}{\rho}\cos\left(\frac{b_1t'}{2a_1}-\frac{4\Omega z}{v_0'}\right), \tag{C5}$$

$$\int_{-\infty}^{+\infty}\omega\,d\omega\,e^{i\omega t'}H_0^{(2)}(\rho A_\pm)e^{\mp i(4\Omega z/v_0')}=\frac{2\sqrt{i}b_1}{(a_1)^{3/2}}\frac{e^{\rho\sqrt{b_1^2/4a_1+c_1}}}{\rho}\sin\left(\frac{b_1t'}{2a_1}-\frac{4\Omega z}{v_0'}\right), \tag{C6}$$

$$\int_{-\infty}^{+\infty}\omega^2 d\omega\,e^{i\omega t'}H_0^{(2)}(\rho A_\pm)e^{\mp i(4\Omega z/v_0')}=\frac{b_1^2}{\sqrt{i}(a_1)^{5/2}}\frac{e^{\rho\sqrt{b_1^2/4a_1+c_1}}}{\rho}\cos\left(\frac{b_1t'}{2a_1}-\frac{4\Omega z}{v_0'}\right), \tag{C7}$$

$$\int_{-\infty}^{+\infty}\omega\,d\omega\,e^{i\omega t'}H_0^{(2)}(\rho A'_\pm)A'_\pm e^{\mp i(2\Omega z/v_0')}e^{\mp\pi i/2}=\frac{-i^{3/2}b_1}{a_1^{3/2}}\left(\frac{b_1^2}{16a_1}+\frac{c_1}{4}\right)^{1/2}\frac{e^{\rho\sqrt{b_1^2/16a_1+c_1/4}}}{\rho}\times\cos\left(\frac{b_1t'}{4a_1}-\frac{2\Omega z}{v_0'}\right), \tag{C8}$$

and

$$\int_{-\infty}^{+\infty}d\omega\,e^{i\omega t'}H_0^{(2)}(\rho A'_\pm)A'_\pm e^{\mp i(2\Omega z/v_0')}e^{\mp\pi i/2}=\frac{4i^{1/2}}{\sqrt{a_1}}\left(\frac{b_1^2}{16a_1}+\frac{c_1}{4}\right)^{1/2}\frac{e^{\rho\sqrt{b_1^2/16a_1+c_1/4}}}{\rho}\sin\left(\frac{b_1t'}{4a_1}-\frac{2\Omega z}{v_0'}\right). \tag{C9}$$

Using the integrals (C2) and (C5)–(C9) we evaluate all the integrals appearing in Eqs. (32)–(34) and obtain the final result given by Eqs. (35)–(37).

[1] S. Schneider and R. Spitzer, Nature (London) **250**, 643 (1974).
[2] S. Schneider and R. Spitzer, Can. J. Phys. **55**, 1499 (1977).
[3] S. Schneider and R. Spitzer, Appl. Phys. **13**, 197 (1977).
[4] S. Schneider and R. Spitzer, IEEE Trans. Microwave Theory Tech. **MTT-25**, 551 (1977).
[5] S. Schneider and R. Spitzer, Phys. Quantum Electron. **5**, 301 (1978); **5**, 347 (1978).
[6] S. Schneider and R. Spitzer, Phys. Quantum Electron. **7**, 323 (1980).
[7] W. W. Zachary, Phys. Quantum Electron. **7**, 779 (1980).
[8] N. M. Kroll, Phys. Quantum Electron. **7**, 355 (1980).
[9] J. Soln, Phys. Rev. D **18**, 2140 (1978).
[10] W. W. Zachary, Phys. Rev. D **20**, 3412 (1979).
[11] A. A. Risbud and R. G. Takawale, J. Phys. A **12**, 905 (1979).

[12] W. Becker, Phys. Rev. A **23**, 2381 (1981).
[13] A. A. Risbud, J. Phys. A **20**, 2743 (1987).
[14] I. Frank and Ig. C. R. Tamm, Acad. Sci. URSS **14**, 109 (1937).
[15] J. Jelley, *Cherenkov Radiation* (Pergamon, London, 1958), p. 21.
[16] V. P. Zrelov, *Cherenkov Radiation in High Energy Physics* (Atomitzdat, Moscow, 1968), Parts I and II.
[17] V. M. Arutyunyan and S. G. Oganesyan, Usp. Fiz. Nauk [Phys. Usp. **37**, 1005 (1994)].
[18] V. M. Harutunia and S. G. Orgenesyn, Phys. Rep. **270**, 217 (1996).
[19] The name is rather misleading due to the word ''stimulated'' and so there were many objections (e.g., [8]) to this name, with which we agree; but we use it here for convenience.
[20] Here the presence of a medium of dielectric constant ϵ (which is greater than 1) causes greater frequency upshift than in the vacuum situation [9].
[21] P. Penfield and D. S. Hermann, *Electrodynamics of Moving Media* (MIT Press, Cambridge, MA, 1967), p. 114.
[22] L. D. Landau, E. M. Lifshitz, and L. P. Pitaevskii, *Electrodynamics of Continuous media*, 2nd ed. (Pergamon, Oxford, 1984), p. 262.
[23] I. M. Frank, Yad. Fiz. **7**, 1100 (1968) [Sov. J. Nucl. Phys. **7**, 660 (1968)].
[24] J. D. Jackson, *Classical Electrodynamics*, 2nd ed. (Wiley, New York, 1975), pp. 522,523,317.
[25] V. M. Arutyunyan and G. K. Avetisyan, Zh. Eksp. Teor. Fiz. **62**, 1639 (1972) [Sov. Phys. JETP **35**, 854 (1972)].
[26] See Appendix A for details of the calculations.
[27] *Handbook of Mathematical Functions*, edited by M. Abramowitz and I. A. Stegun (Dover, New York, 1970).
[28] See Appendix B for details of the calculations.
[29] I. G. Tamm, J. Phys. (Moscow) **1**, 439 (1939); **1**, 446 (1939).
[30] H. Batemann, *Table of Integral Transforms*, Vol. I of Batemann Manuscript Project, edited by A. Erdelyi (McGraw-Hill, New York, 1954), pp. 15,135.
[31] Y. L. Luke, *Integrals of Bessel Functions* (McGraw-Hill, New York, 1962), p. 147.
[32] In our calculations, the parameter μ introduced in Eq. (10) is $(\beta_0 n_0 - 1)$, and it is used in the linearization procedure with $\mu \ll 1$. This ensures that we are considering the region very near the threshold of superphase motion.
[33] See Appendix C for details of integration.
[34] As $(\epsilon \beta_0'^2 - 1)^{-1} \simeq 1/2\mu \gg 1$.
[35] 100 MeV electrons traversing 1 cm of H_2O over a waveband of 4000–5000 Å give a CR yield $\sim$2.7 keV $= 3.3 \times 10^{-23}$ J when the full range $\omega = 0 - 10^{16}$ Hz is taken.
[36] Note that the Lorentz force equation is valid in all inertial frames.
[37] Note that $\mu = (\beta_0 n_0 - 1) \ll 1$.
[38] To ensure $u_y|_{t=0} = 0$, we have to choose $\phi_0 = \pi/2$.
[39] H. Batemann, *Table of Integral Transforms* (Ref. [30]), Vol. II, p. 49.
[40] Here the formulas (11)–(16) of Ref. [39] are used.
[41] Here $\phi' = \pm \pi$ is chosen.